DEPARTMENT OF ENGINEERING

experiments on the control of plane jets by auxiliary flows

J. WUERER

REPORT NO. 63-31

UNIVERSITY OF CALIFORNIA, LOS ANGELES

Report No. 63-31
July 1963

EXPERIMENTS ON THE CONTROL OF PLANE JETS BY AUXILIARY FLOWS

Josef Wuerer

Aerosonics Laboratory
Department of Engineering
University of California
Los Angeles 24, California

FOREWORD

The research described in this report, *Experiments on the Control of Plane Jets by Auxiliary Flows*, by Josef Wuerer, was carried out under the technical direction of Professor Alan Powell and is part of the continuing program in Fluid Motion and Sound.

This project is conducted under the sponsorship of the Fluid Dynamics Branch, Mathematical Sciences Division, Office of Naval Research.

Submitted in partial fulfillment of Contract Number Nonr-233(62), Authority Number NR 062-229.

ABSTRACT

The operation of certain types of fluid flow devices depends upon the character and response of jet flows to applied disturbances. In such devices it is typical for a power jet to be deflected by a laterally impinging control jet, either in a steady or dynamic regime. Two-dimensional jet flows relevant to these devices are studied experimentally as a separate element, i.e., free from the effects of nearby solid boundaries.

Steady deflection characteristics for several jet geometries are discussed and illustrated by photographs. For a single control jet system, flow measurements show a linear relationship between the momenta of the two interacting jets for constant angles of deflection. Analytical expressions which describe the deflection angle and resultant pressure forces in terms of the jet momenta are developed. For two symmetrically placed control jets, it is found that there exists a particular setback of the jet housings where control flow requirements are minimum. The problem of deflection past a wedge centered in the power jet stream is also considered.

Dynamic studies include geometries with and without a wedge present. For moderate disturbances to the free jet, it is found that neutral stability persists at a Strouhal number of about 0.5. Some observations are included for dynamic traverse of the jet past a wedge and also self-excited oscillations with a wedge present.

TABLE OF CONTENTS

LIST OF FIGURES

LIST OF FIGURES (Cont.)

LIST OF SYMBOLS

E	Elevation to bottom of control jet channel (l)
F_X	Resultant force in x-direction (ml/t)
F_Y	Resultant force in y-direction (ml/t)
f	Cycling Frequency (cycles/t)
h	Elevation of wedge (l)
h_c	Critical wedge elevation for self-excited oscillations (l)
J	Momentum flux (ml/t)
J_c	Control jet momentum flux (ml/t)
J_p	Power jet momentum flux (ml/t)
J_1	Momentum flux of component of combined jet due to power jet (ml/t)
J_2	Momentum flux of component of combined jet due to control jet (ml/t)
L	Elevation of control jet assembly at exit plane
l	Fundamental dimension of length (l)
m	Mass (m)
Q_c	Volume flow rate, control jet (l^3/t)
Q_p	Volume flow rate, power jet (l^3/t)
R	Reynolds number (dimensionless)
R_c	Control jet Reynolds number (dimensionless)
R_p	Power jet Reynolds number (dimensionless)
S	Strouhal number (dimensionless)
S_1	Setback of control jet channel base (l)
S_2	Setback of control jet channel top (l)
t	Time (t)
U	Mean velocity (l/t)
W_p	Power nozzle width (l)
W_c	Control nozzle width (l)

LIST OF SYMBOLS (Cont.)

x	Direction parallel to control nozzle axis
y	Direction parallel to power nozzle axis
θ	Final deflection angle of power jet (degrees)
θ_d	Initial deflection angle of power jet (degrees)
θ_w	Half wedge angle (degrees)

I. INTRODUCTION

Early in 1960 the development of a new class of fluid flow devices, typified by the fluid amplifier, was announced.[1] Since that time considerable effort has been made to integrate fluid jet devices into logic systems owing to their extreme physical simplicity and high reliability.

The operation of most fluid jet control elements is centered around the ability of a higher energy fluid stream (the power jet) to be deflected by a stream of lower energy (the control jet). Most elements employ rectangular nozzles giving nearly two-dimensional flows.

Along with the development of these devices a new group of quite complex fluid flow problems have emerged. To date, singularly few characteristics of the flows involved have been predicted by entirely theoretical reasoning, or even with the aid of experimental observation of that type so typical to fluid dynamics. Most progress has been solely along empirical lines and hence has failed to yield general results.

In particular, the lack of an adequate theory explaining the behavior of submerged interacting jets is one of the major problem areas.[2] This aspect is precisely the point of concentration for the present study. To gain insight into the phenomena associated with the jet flows the most simple situation is taken, i.e., the complicated (although admittedly important) effects of sidewalls adjacent to the issuing power jet are deliberately avoided. Attention is limited to incompressible and more or less laminar two-dimensional flows.

The present work represents part of a broader program to study the behavior of interacting fluid jets. A more detailed account of certain experimental aspects of the present study is described elsewhere by Wuerer.[3] The general nature of the problem together with some early experimental results were presented in a paper by Powell.[4] The problem of jet control with extended sidewalls is presently being investigated.[5]

II EQUIPMENT

The essential features of the test apparatus were the power jet and control jet assemblies, the latter directing the input to produce special effects

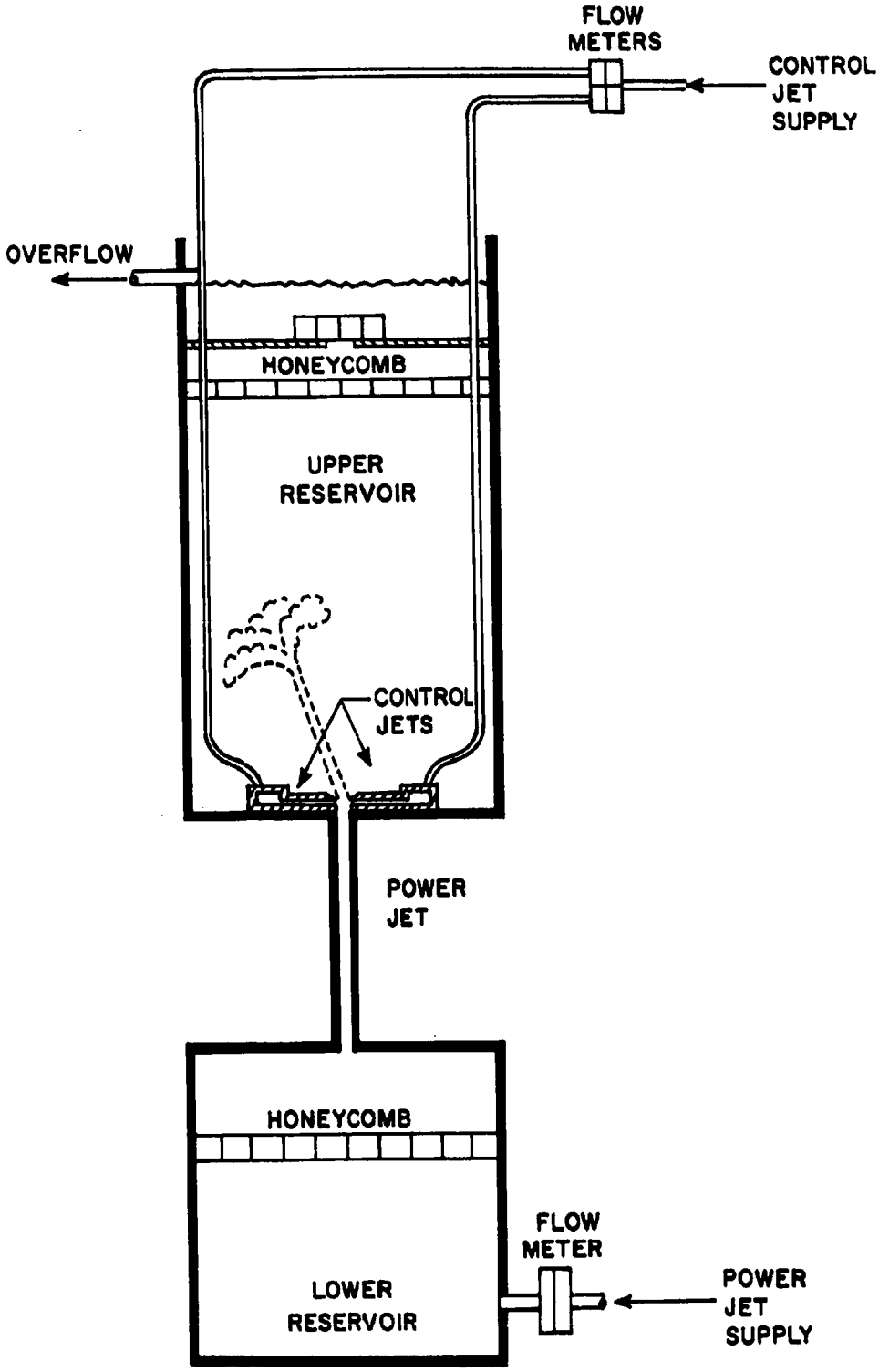

LAYOUT OF TEST EQUIPMENT

FIGURE 1

on the power jet. A layout of this equipment is shown schematically in Figure 1.

The power jet system basically was made up of three elements: a settling chamber, nozzle, and discharge reservoir. The nozzle, rectangular in shape, was 7 inches long, 1/4 inch wide and 6 inches deep. The entrance was faired to minimize turbulence effects and the exit was square and set flush with the floor of the upper tank, in which a fluid level of about 15 inches was maintained. The discharge was vertical so as to prevent lateral deflection due to buoyancy effects. Sections of aluminum honeycomb were placed in both the upper and lower tanks to decrease the tendency for circulatory flows to become established.

The control jets were constructed as removeable units to allow their convenient positioning in various locations with respect to the power jet exit. The nozzle length was 2-5/8 inches having the same depth as the power jet, 6 inches. The nozzle width was 0.020 inch. The supply chamber to the nozzle was 1/2 inch by 3/8 inch in cross-section and extended the full depth of the unit.

The working fluid, water, was supplied to the system from a 55 gallon constant head reservoir. A fluid level of about 8 feet above the exit plane of the power jet was maintained. Water temperatures remained quite constant after equilibrium conditions were reached. Changes were of the order of 1 degree F per hour, indicating that any temperature gradients would be very small.

Flow control for each jet was regulated through appropriately sized needle valves and flowmeters. A separate rotary valve device was constructed to provide periodic control flows. The shape of the output was approximately a square wave and cycling speeds up to 400 cycles per minute could be obtained.

Essential parts of both the power and control jet assemblies were constructed from lucite to allow flow visualization, which was accomplished by dye injection. Three 0.010 inch hypodermic tubes were positioned in the power jet nozzle so as to define the boundaries and the centerline of the jet efflux. For visualization of the control flow, dye was injected in the supply line faintly coloring the entire jet efflux.

Both power and control jet nozzles were designed so that velocity profiles across the width at the exit plane would be parabolic for all experimental values of R. On the other hand the depth of the nozzles was great enough that profiles were quite two-dimensional. It was estimated that the boundary layers on the nozzle endwalls stretched less than 10% of the distance between them, even for the lowest values of R.

III. CHARACTERISTICS OF THE STEADY SUBMERGED JET

The steady two-dimensional laminar jet is one of the few flow problems which has been solved explicitly and exactly, even though this concerns the flow from an infinitely narrow slit.[6] For this flow the cross-sectional velocity profiles are similar, having the shape of the square of the hyperbolic secant. There is a decay in centerline velocity, which varies like $x^{-1/3}$, x being the downstream distance measured from the orifice. The corresponding spread of jet width varies like $x^{2/3}$ so that the momentum flux of the issuing jet remains constant.

The analogous problem has also been solved for the case of turbulent flow using Prandtl's hypothesis for shear.[7] Here again the velocity profile for a given cross-section varies like the sech^2 of the ordinate, but the decrease in centerline velocity and increase in jet width vary like $x^{-1/2}$ and x respectively.

In practice, the jet must emerge from a slit of finite width, hence, a transitional region exists before the real velocity profile assumes the shape predicted by theory. Experimental results show that, unfortunately, this transitional region occupies that part of the flow of greatest interest in the present study, say up to a distance of ten slit widths from the exit.[8, 9] Nevertheless, the existence of an explicit solution has proved to be a useful tool especially in allowing theoretical progress in the very important and highly relevant question of jet stability which will be discussed later.

In the present experiments theoretical velocity profiles were additionally altered due to the presence of the finitely spaced tank sidewalls. A weak downward flow near the outer edge of the tank resulted due to flow entrainment by

the viscous jet. However, it is very unlikely that conditions within several slit-widths from the orifice and especially near the jet centerline would be appreciably affected. Hence, even though certain restrictions exist, analytical results should at least give a reasonable first approximation.

Throughout the range studied, $80 < R < 430$, the issuing jet appeared quite laminar up to a distance of at least four slit-widths. Beyond this distance specific characteristics of the jet were greatly dependent on R. For $80 < R < 200$ the resultant flow remained laminar up to about 16 slit-widths. Beyond this point wavy irregularities attributed to random disturbances were noted. These irregularities were rapidly amplified into a highly irregular undefined motion, Figure 2. It is to be realized, of course, that the fluid bounded by the dye lines represents the efflux from the orifice only, and not the entire flow field of the jet. At the upper flow limit, $R = 420$, laminar flow persisted for about 4 slit-widths followed by small disturbances which developed into a more defined region of turbulence at about 10 to 12 slit-widths, Figure 3. For R between the above two limiting values jet characteristics changed gradually.

IV. DIRECTIONAL CONTROL BY STEADY SIDE JETS

A fluid jet may be deflected by imparting lateral momentum to it by means of an impinging side jet. This may be accomplished by many geometrical arrangements. Several of the possible variables are indicated in Figure 4. In the present experiments, setback (dimension S) was the only variable. The other dimensions were held constant and were $W_p = E = 0.25$ inch, $W_c = 0.08\ W_p$, and $L = 5/16$ inch.

The first study was for the case of deflection by a single control jet with zero setback. This geometry is shown in Figure 5. When the control jet was inactive, the physical presence of the mechanism had no effect on the resultant direction of the power jet. The issuing fluid continued in its original axial direction. The introduction of flow through the control channel immediately resulted in a noticeable deflection of the main stream in the direction of the control flow.

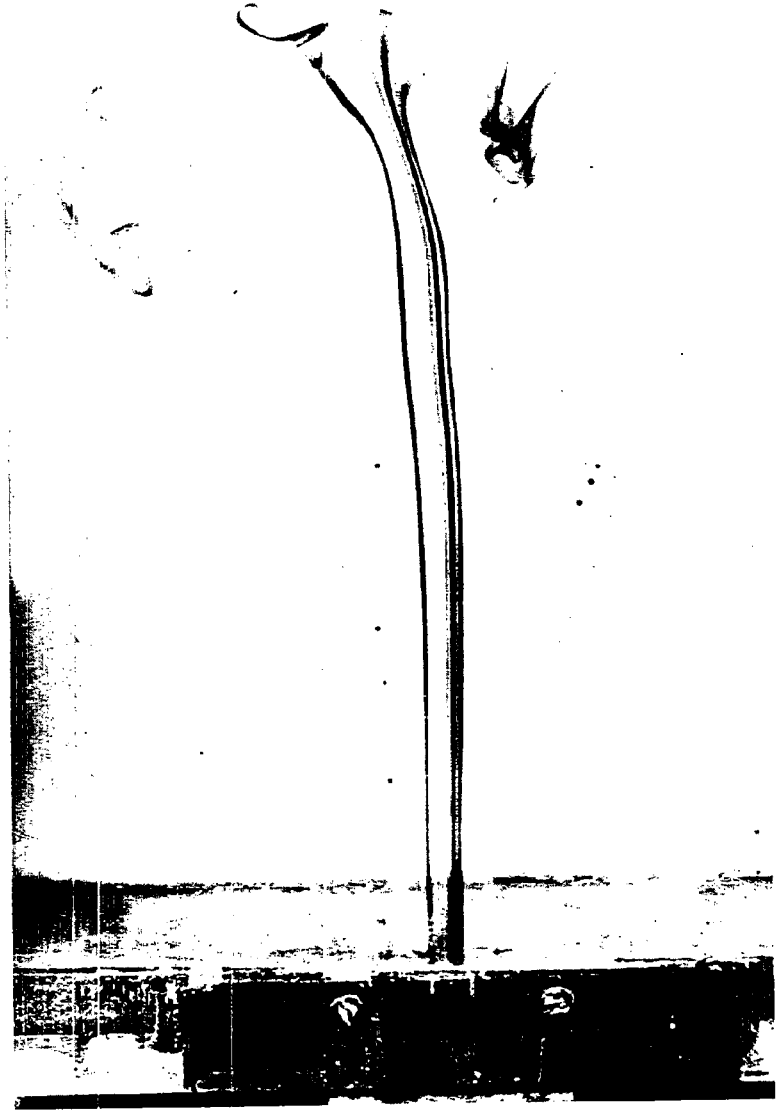

FIGURE 2

Free Jet, R = 200

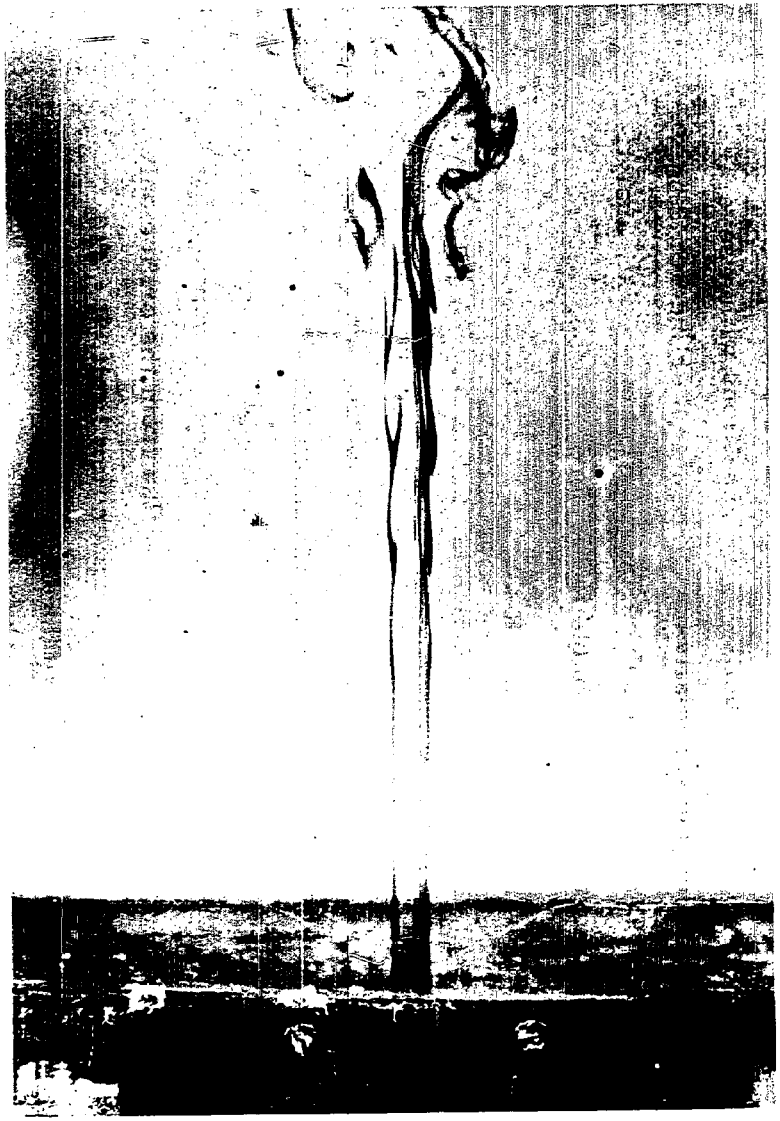

FIGURE 3

Free Jet, R = 420

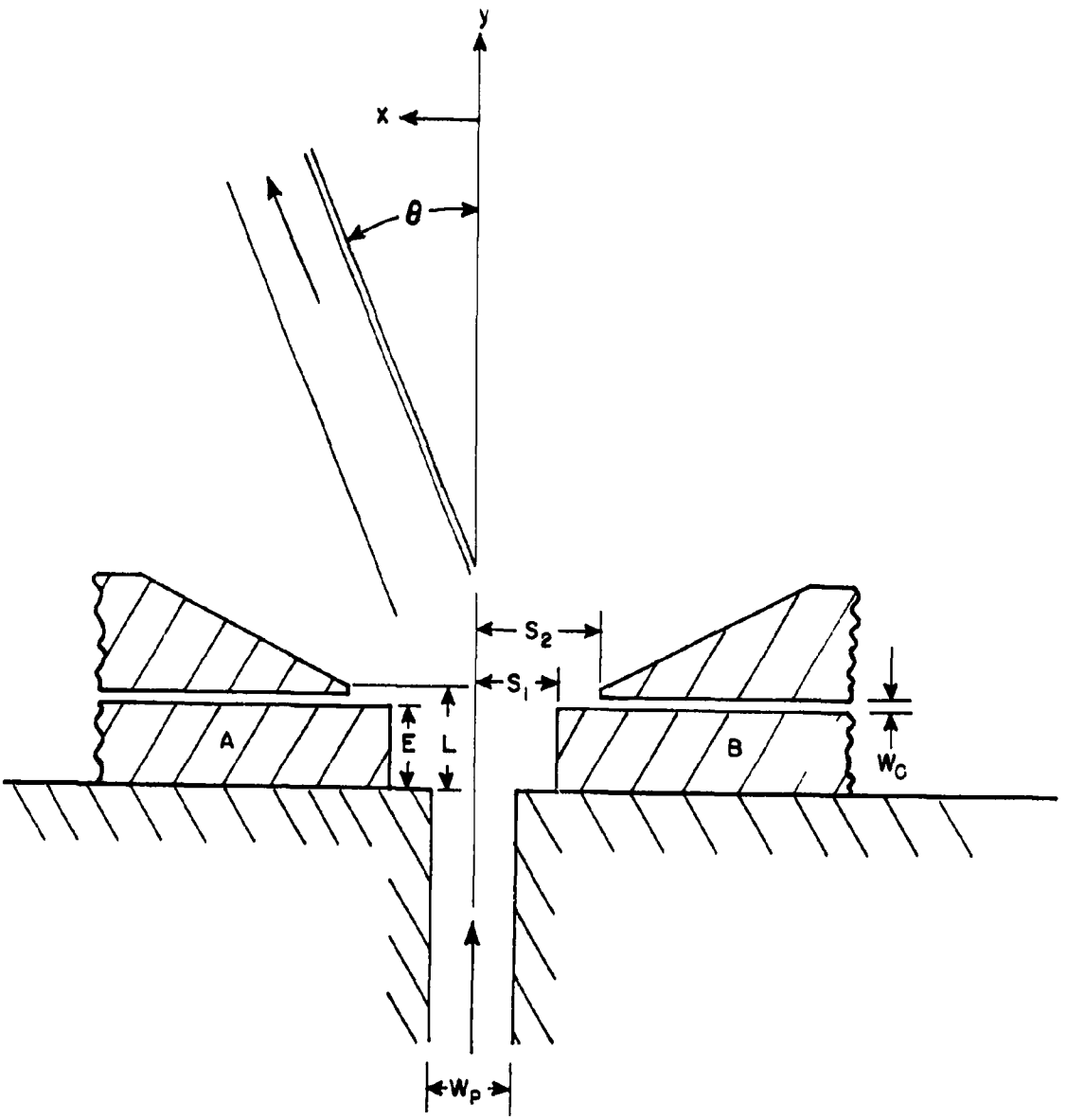

SYMMETRICAL CONTROL JET DEVICE,
REFERENCE DIMENSIONS INDICATED

FIGURE 4

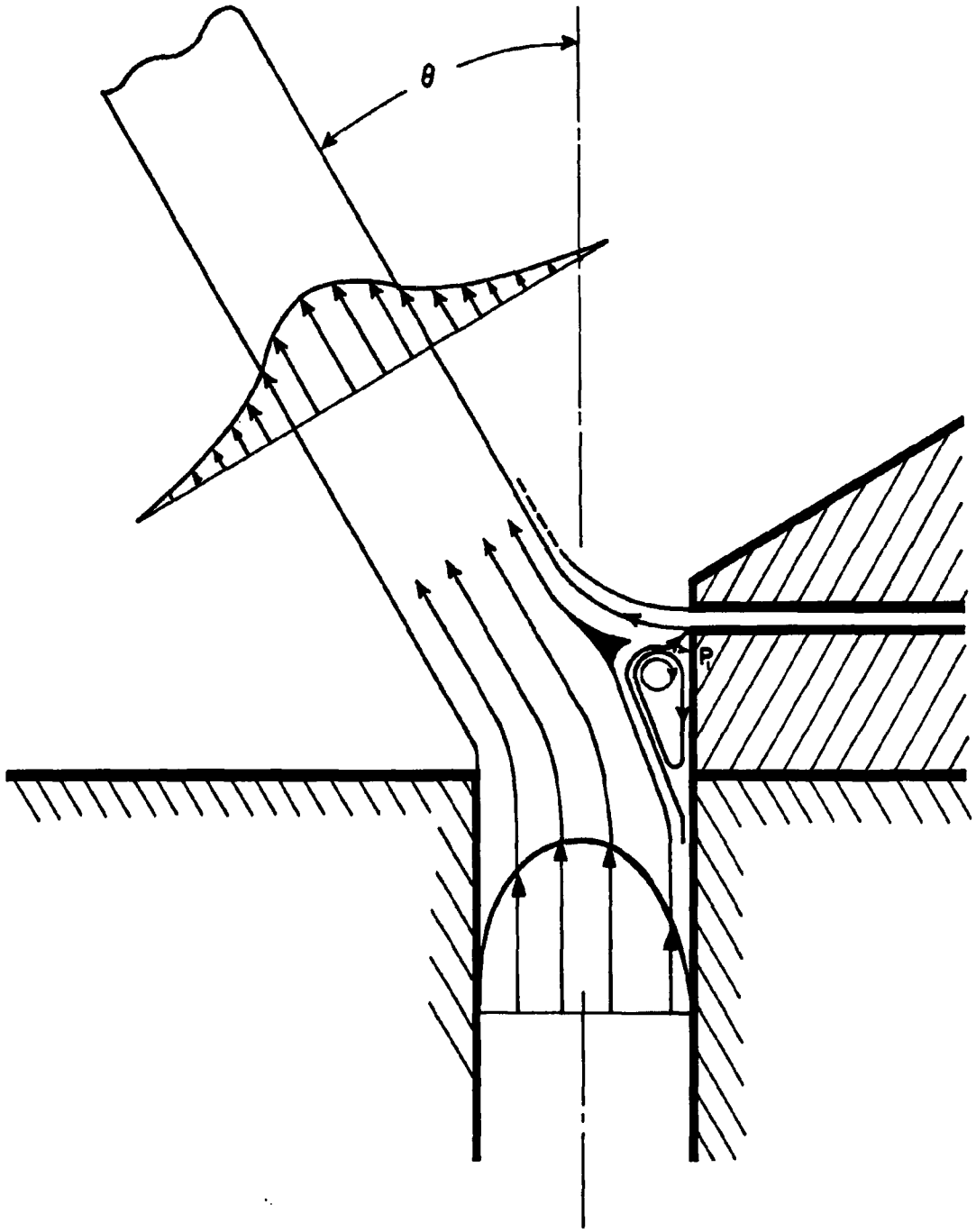

RESULTANT FLOW PATTERN, DEFLECTION BY A SINGLE CONTROL JET, ZERO SETBACK

FIGURE 5

The condition of the deflected flow was greatly dependent on the flow rates of both jets. Two extremes for a particular angle of deflection, 30 degrees, are shown in Figures 6 and 7. For reasonable deflection, up to about 45 degrees, the condition of the resultant deflected flow was similar to that described previously for the undistrubed flow, excepting perhaps a slight reduction in the length of completely laminar activity. As deflection was increased past about 50 degrees the extent of the region of laminar flow became greatly reduced.

The individual flows from each nozzle remained distinct in the immediate neighborhood of impingement, as shown in Figure 5, and remained so at least in the region of laminar flow and incipient transition to turbulence. After impingement, the distance between adjacent streamlines of issuing fluid were somewhat narrowed, indicating an increase in velocity. This characteristic was exhibited by both streams. It must be realized, however, due to the effect of jet spreading previously discussed, that the jet motion is not limited only to the issuing fluid within the dyed or observable boundaries. Hence, it cannot be deduced directly what result the narrowing may have on resultant velocity profiles.

Close to the point of intersection of the two jets, an eddy motion always persisted whenever flow emerged from the control channel, deflecting the power jet. This motion can be seen in Figures 6 and 7. A typical enlargement of this area is drawn in Figure 5, where the streamlines are based on magnified visual observations. The eddy region is completely entrained by the fluid of the power jet and adjacent segment of vertical wall.

The flow separation and eddy formation shown are attributed to the result of the adverse pressure gradient established along the wall due to the impinging jets and viscous effects. The observed flow pattern, i.e., the stagnation point (P_1 in Figure 5) and apparent slowing down of the flow, indicated that the pressure in the eddy was greater than the ambient pressure. Qualitative tests observing the flow established through a small pressure tap on the wall confirmed this point.

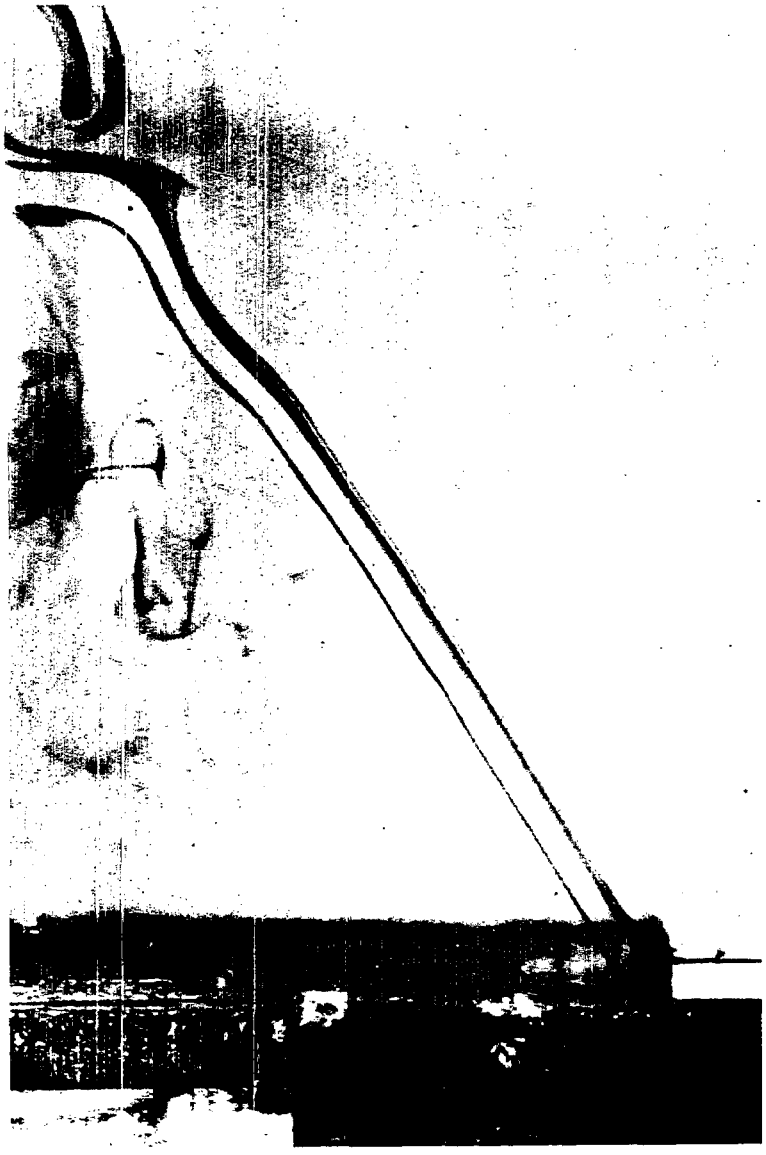

SINGLE CONTROL JET ZERO SETBACK
$R_p = 165$, $R_c = 26$, $\theta = 30^o$
FIGURE 6

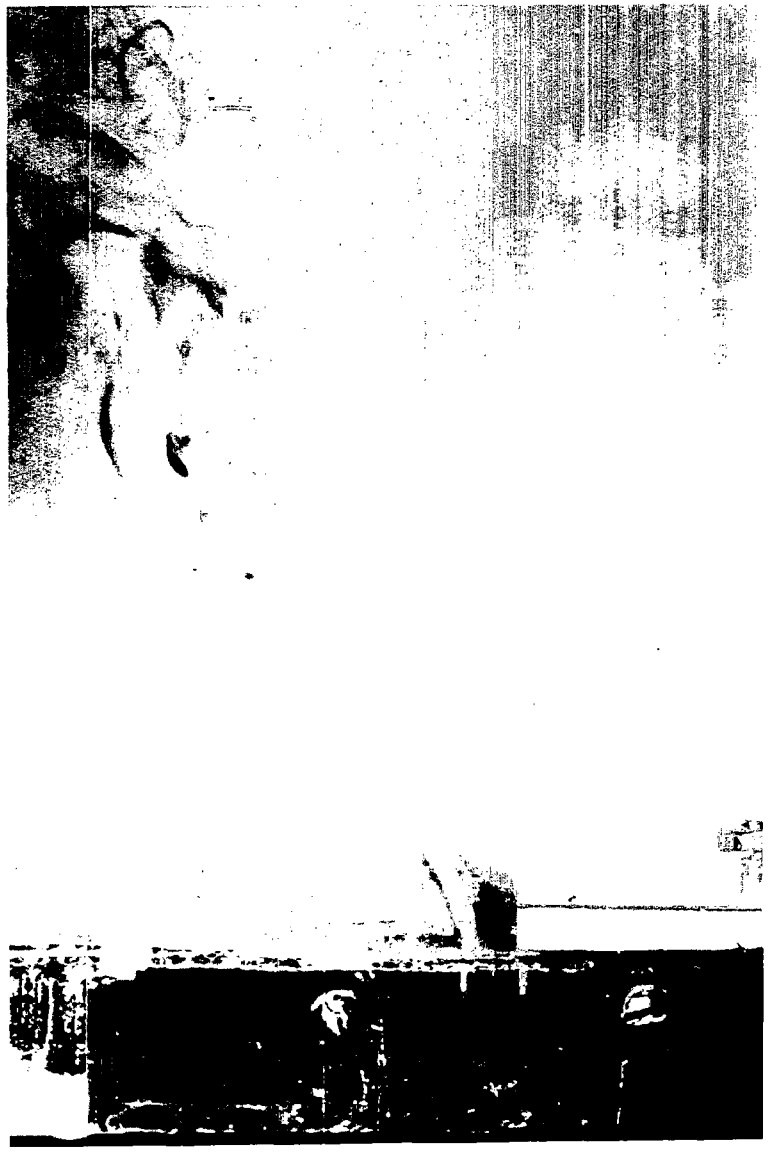

SINGLE CONTROL JET ZERO SETBACK
$R_p = 420$, $R_c = 61$, $\theta = 30^o$
FIGURE 7

Results for the case of zero setback are plotted in Figure 8 which shows the relationship of the deflection angle to the momentum flux of the power and control jets. It is found that the dependence of the power and control jet momentum requirements to maintain a constant deflection angle is linear. An unresolved peculiarity of the plot is that the projections of the lines from the lower experimental limit do not converge on the origin, a point that each curve would be expected to tend toward. Instead, the lines focus slightly to the left of the origin. At first glance, an error in flow measurements might be suspected; however, careful metering checks indicated no errors of the magnitude required to shift the point of convergence. Consequently, the region between the lower limit of experiment and the origin (i.e., very small flows) remains somewhat undefined. Because of the great effect of even weak tank currents on very slow flows no reliable experimental work could be carried out to fill this gap.

Resultant flows for finite setback of a single control jet were somewhat different than for zero setback, especially in the absence of control flow. For the particular geometry described, for setbacks up to 1/8 inch, a significant deflection of the power jet was noted when the control jet was inactive, Figure 9. In certain cases deflections up to 15 degrees in the direction of setback were noted.

The general tendency for a fluid jet to attach to a nearby adjacent wall (Coanda effect[10]) has been the object of considerable study. The cause of the phenomenon here is attributed to the acceleration of fluid entrained by the jet as it is drawn into the setback cavity. This increase in velocity results in a corresponding decrease in pressure in the cavity causing a net force on the jet toward the wall. Several investigators have treated the subject both experimentally and analytically.[11, 12, 13, 14]

When the momentum of the control jet was increased sufficiently to overcome the negative deflection, a flow pattern similar to that in Figure 5 prevailed. However, the cross-sectional area of the eddy was greater, its width being increased approximately by the setback distance. As the setback

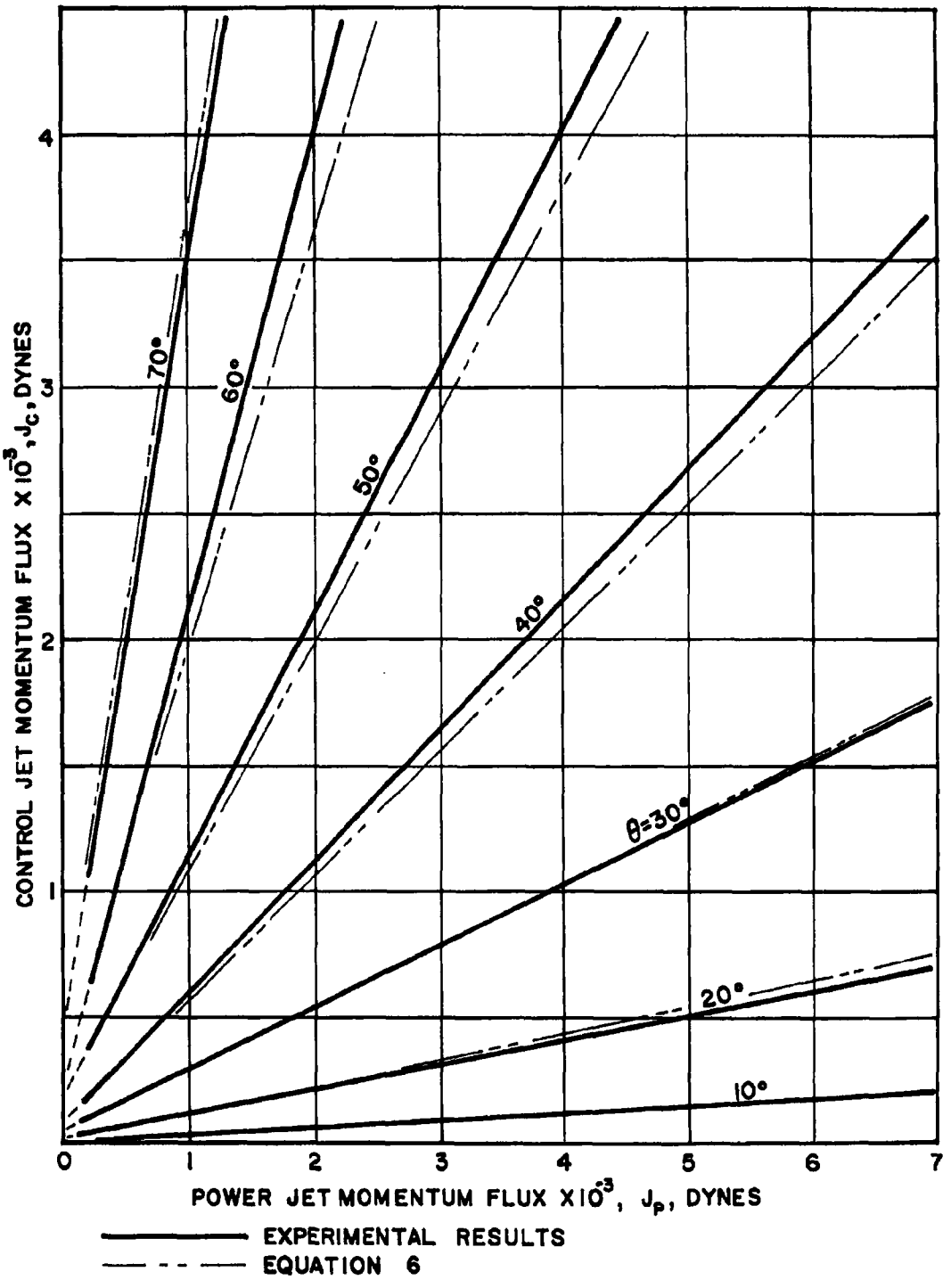

DEFLECTION BY A SINGLE CONTROL JET, ZERO SETBACK

FIGURE 8

distance approached about 5 control nozzle slit-widths, the tendency existed for the impinging control jet to become unstable and oscillate laterally. This motion consequently resulted in the transmission of periodic disturbances to the deflected power jet. This condition is shown in Figure 10.

A third single-jet geometry was considered, namely the case where only the top of the control jet channel was setback, S_2 = 1/8 inch, S_1 = 0, Figure 4. The flow pattern in the interaction region was virtually unchanged from the case of zero setback, Figure 5. No negative deflection was observed for zero control flow due to the very short length of the adjacent wall, the distance L-E, Figure 4.

Deflection characteristics for the various amounts of setback studied were quite similar to those shown for zero setback in Figure 8. However, control flow requirements to achieve the same deflection angle increased. This tendency may be seen by comparing curves 3, 4, and 6 in Figure 11, which shows the relative flow requirements for several jet geometries for θ = 20 degrees.

In contrast to the single-jet geometries, Figure 4 shows a typical symmetrically opposed control jet arrangement. With this scheme the power jet may be deflected in both directions either by one of the two control jets or by the differential flow of two active control jets. Only the first case was studied in the present experiments.

For the symmetrical configuration, the characteristics of the power jet in the absence of control flow were very similar to those previously described. The only major difference in the flow for the present case resulted from setback effects. When the control jet assemblies were set flush with the power channel walls, the result was merely to extend the walls, the efflux being similar to that shown in Figures 2 and 3. However, as soon as the setback was made finite a noticeable spreading of the power jet occurred, Figure 12. For this geometry two low pressure regions exist, one in each setback cavity. The higher pressure at the jet center results in a spreading action. As the setback distance was further increased a certain point was reached (about 1/16 inch) where the tendency for spreading decreased. For

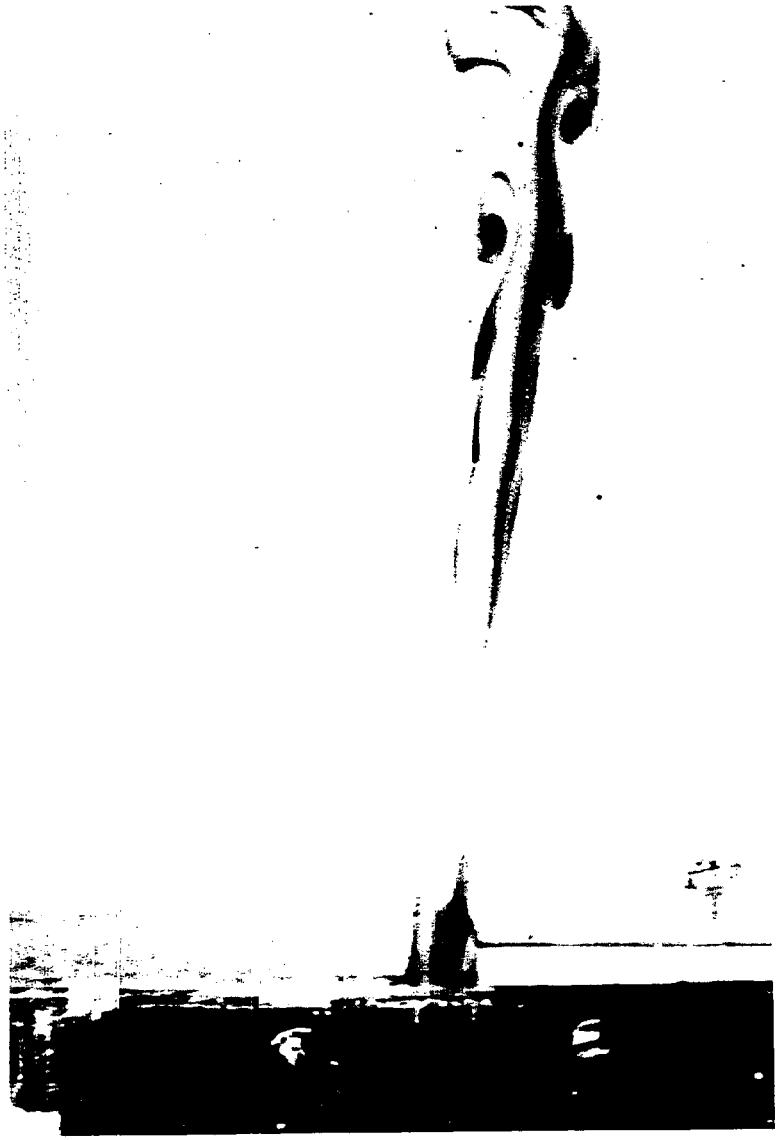

SINGLE CONTROL JET 1/16 INCH SETBACK
$R_p = 282$, $R_c = 0$, $\theta = -8^o$
FIGURE 9

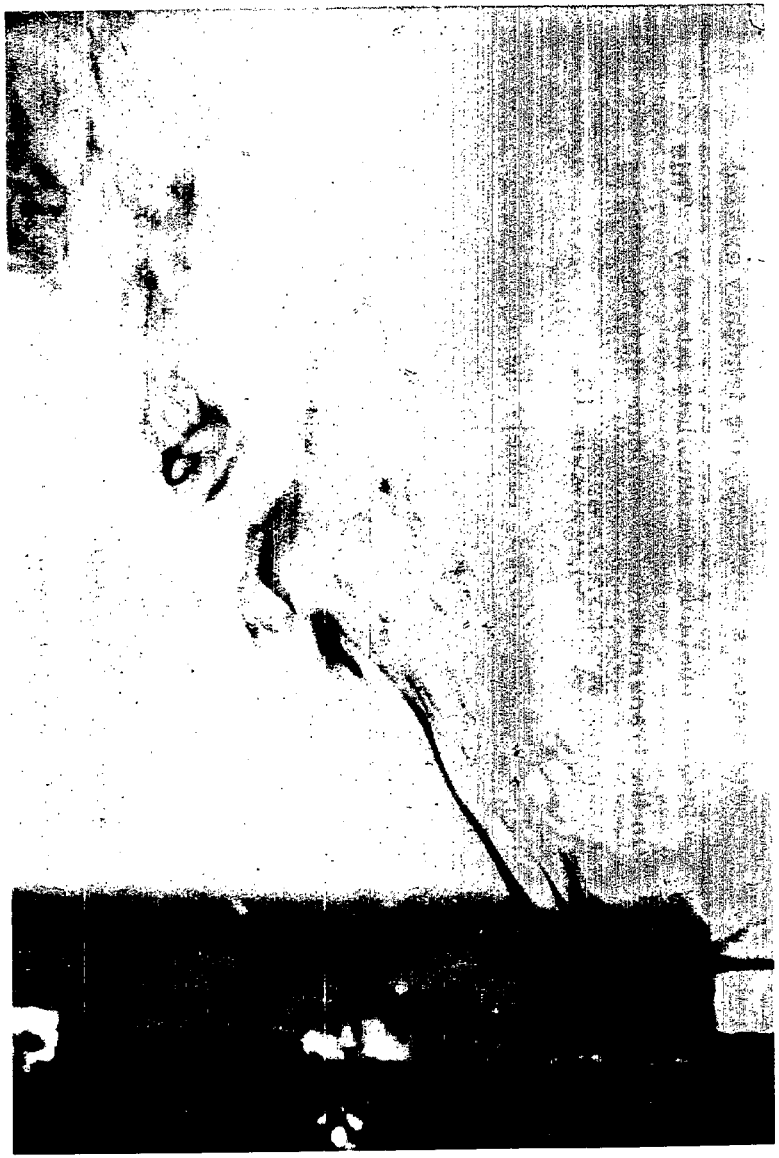

SINGLE CONTROL JET 3/16 INCH SETBACK
$R_p = 282$, $R_c = 65$, $\theta = 30^o$
FIGURE 10

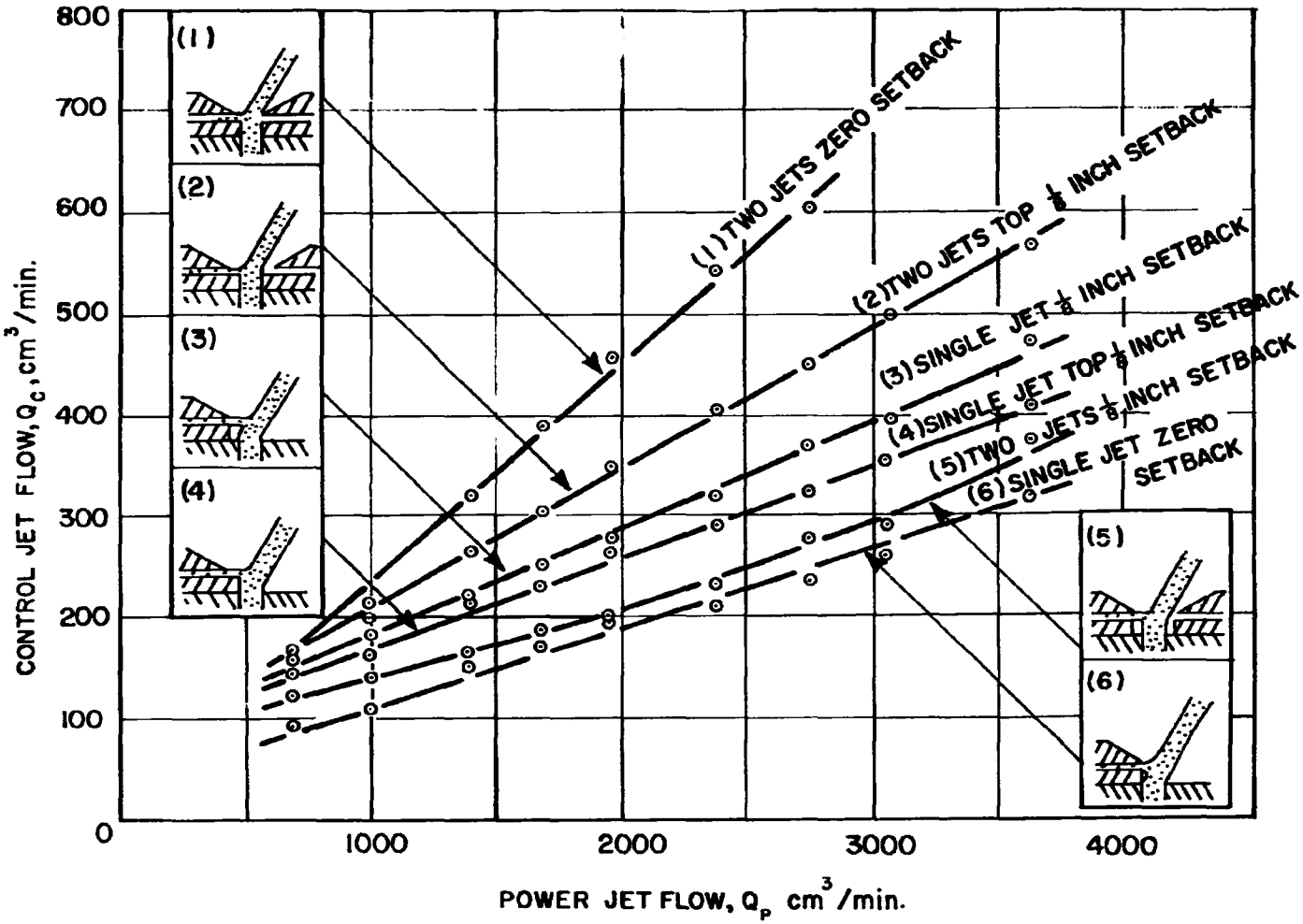

CONTROL FLOW REQUIREMENTS FOR SEVERAL JET GEOMETRIES, θ = 20 DEGREES

FIGURE 11

distances greater than about 3/16 inch, there was essentially no spreading of the observable boundaries due to setback.

The presence of the second (inactive) control jet assembly clearly impedes the deflection of the power jet by the active control jet. Furthermore, the confined flow from the control jet causes a considerable narrowing of the power jet. This situation may be seen in Figure 13 where there is about a 30 percent reduction of the jet width. With this geometry the control jet flow must be more than doubled to achieve the same deflection as when only one control jet is present, curves 1 and 6, Figure 11.

The flow constriction caused by the pair of control jets may be relieved partially by setback of the upper lip of the control nozzles. This may be seen by the comparison of curves 1 and 2, Figure 11. However, the flow requirements for this case are still considerably greater than for the analogous single jet configuration, curve 3.

Uniform setback of the control jets further reduced the flow constriction. However, if the setback was increased greatly the flow requirements again increased due to the lesser effectiveness of the active control jet. The question naturally arises as to what amount of setback results in minimum control flow requirements. That there exists such an optimum condition is indicated in Figure 14, which shows the variation in control flow requirements, for several power jet flow rates and setback distances, to maintain a constant flow deflection of 20 degrees. It is also to be noted that the flow requirements at this optimum condition (about 1/8 inch setback), curve 5, Figure 11, compare favorably with the case for the single-jet with zero setback, curve 6, which was the most efficient geometry.

Analytically, the problem of submerged interacting viscid fluid jets is extremely difficult. Even for inviscid flow, the most simple case, that of impinging free jets, is in general indeterminate.[15] The present problem is beset by additional complexity due to the presence of solid boundaries.

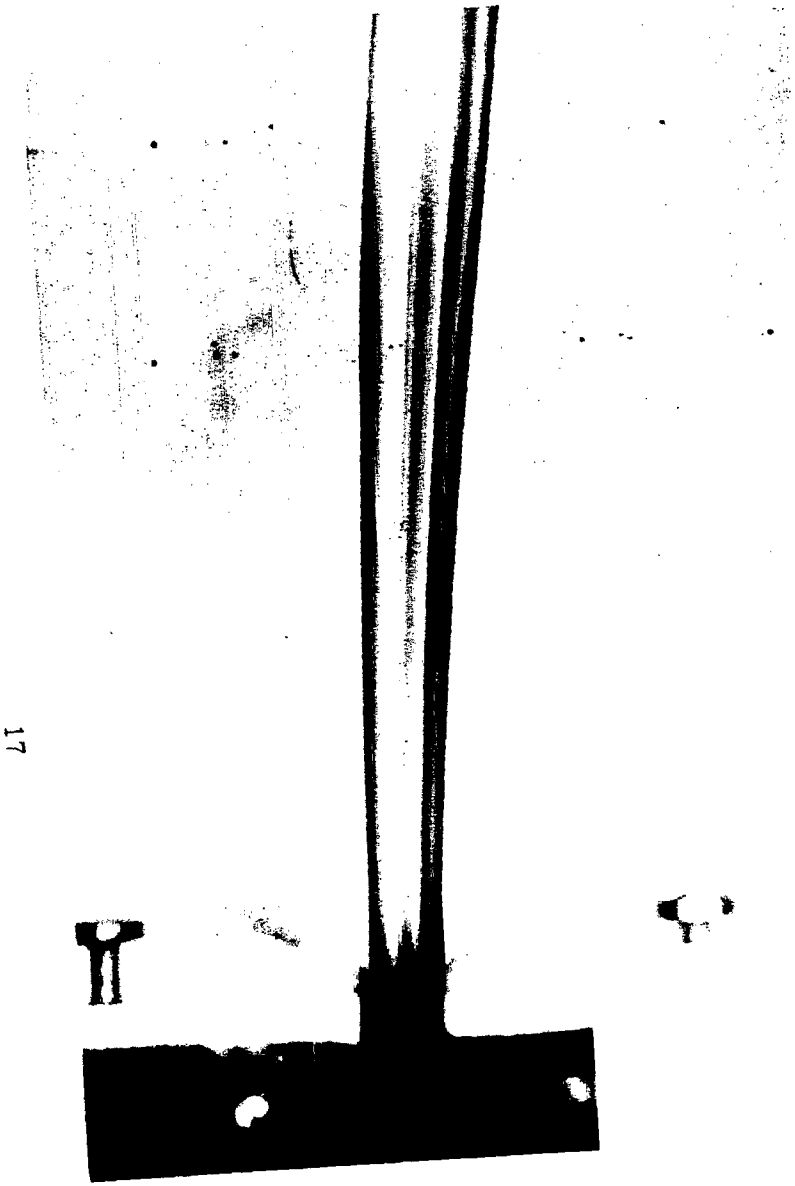

TWO CONTROL JETS 1/16 INCH SETBACK
$R_p = 118$, $R_c = 0$, $\theta = 0^o$
FIGURE 12

TWO CONTROL JETS ZERO SETBACK
$R_p = 326$, $R_c = 72$, $\theta = 20^o$
FIGURE 13

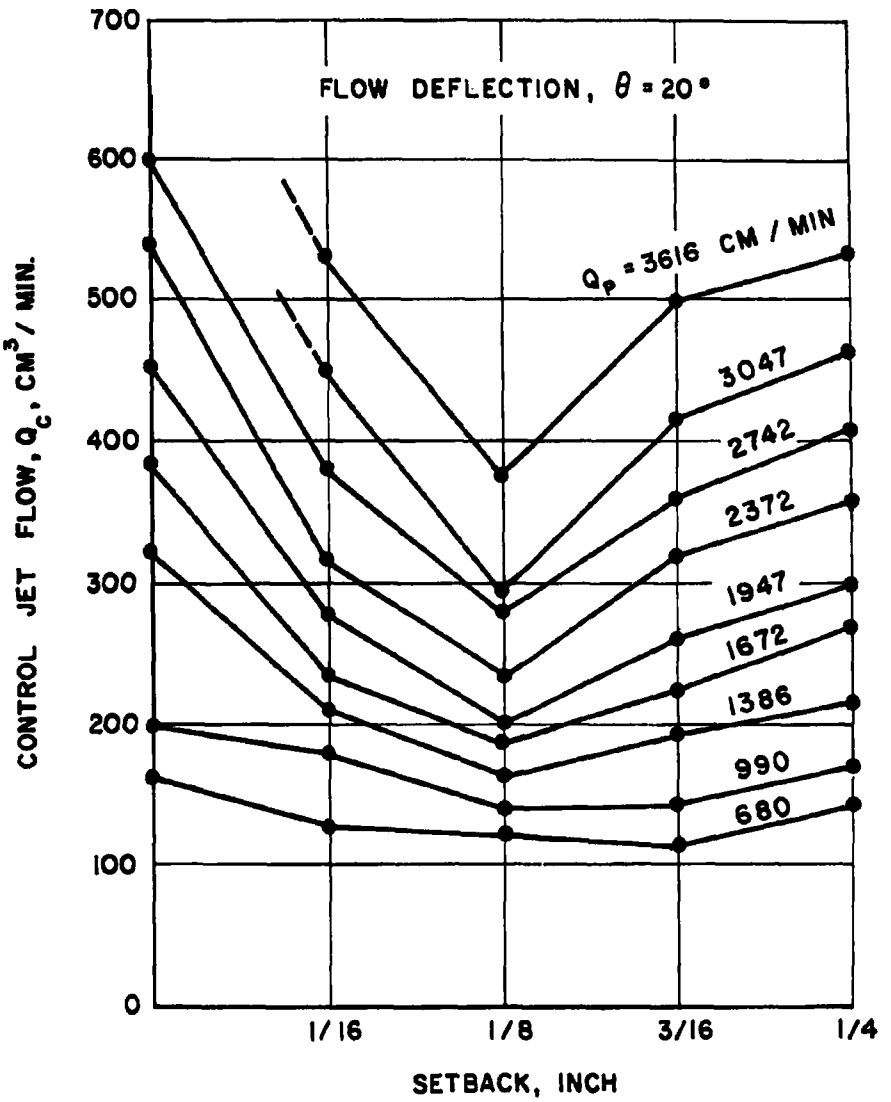

CONTROL FLOW REQUIREMENTS vs. SETBACK

FIGURE 14

For an approach to the present problem, a simplified inviscid flow model based partially on the observed flow was developed, Figure 15. The forces thought to be significant are indicated. A description of these forces is as follows:

(1) F_1, F_2, and F_3 represent pressure distributions caused by the tendency of the constraining walls to resist jet deflection. These resultant forces are in the directions indicated by the respective arrows since the reaction can only be normal to the surface.

(2) F_4 and F_5 represent net force distributions on the jet resulting from a lowering of the pressure in the regions indicated due to fluid entrainment (Coanda effect).

(3) F_6 is a force resulting from the impingement characteristics of the two jets in the presence of an adjacent wall. Here, the flow is slowed down resulting in a pressure increase. Indications are that this force is greatest for zero setback.

Momentum equations may now be written as follows.

<u>y - component:</u>

$$J_p - F_3 - F_{4_y} - F_{5_y} = (J_1 + J_2)\cos\theta \tag{1}$$

<u>x - component:</u>

$$J_c - F_1 - F_2 + F_{4_x} + F_{5_x} + F_6 = (J_1 + J_2)\sin\theta \tag{2}$$

For the case of only one control jet present, the above equations may be considerably simplified. First of all F_1, F_4 and F_5 are non-existent. Secondly, since the control jet issues almost parallel at the channel exit, (Figures 5, 6, 7), it is reasonable to assume that $F_3 \simeq 0$. Hence, it follows that for this case we may write for the

y - component of the momentum:

$$J_p = (J_1 + J_2)\cos\theta \tag{3}$$

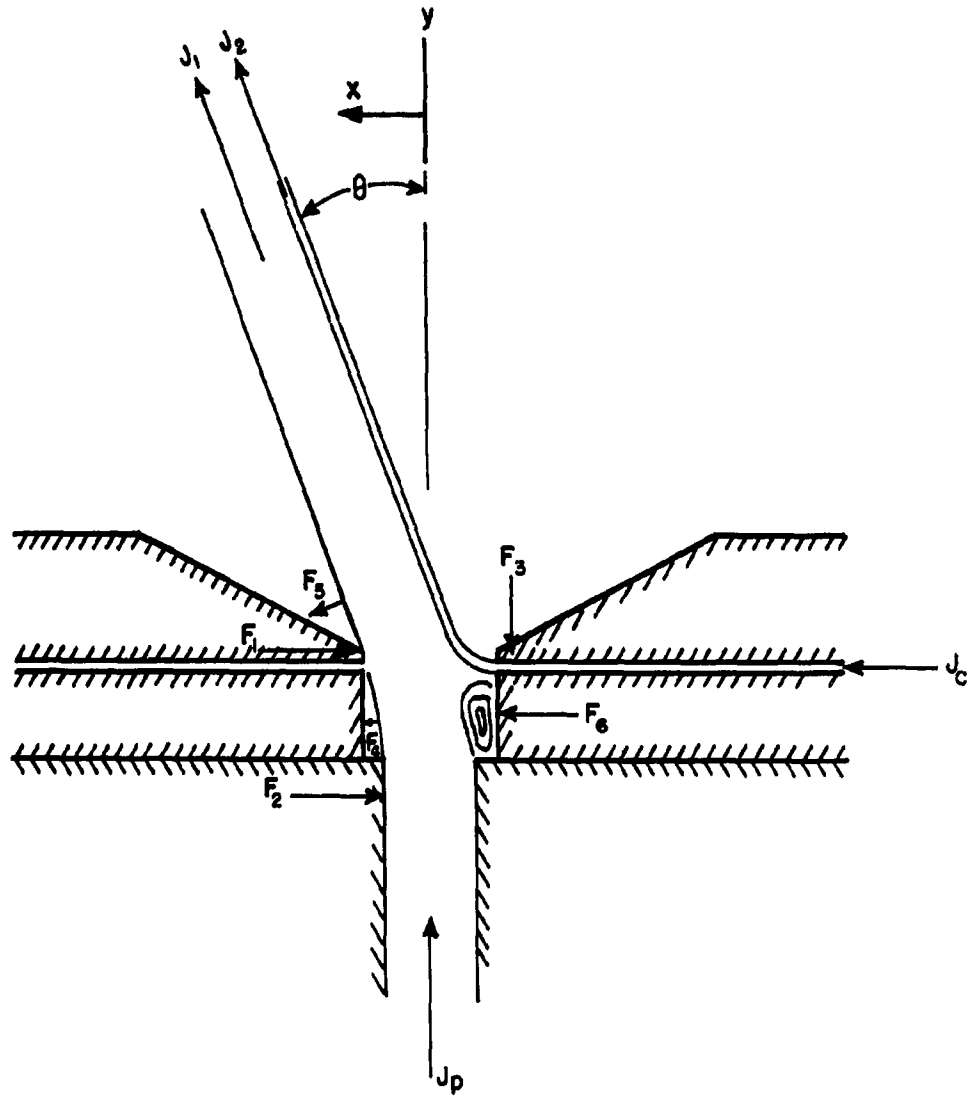

INVISCID MODEL FOR JET DEFLECTION BASED ON OBSERVED FLOW

FIGURE 15

while for the

x - component:

$$J_c = F_2 - F_6 + (J_1 + J_2)\sin\theta = \sum F_x + (J_1 + J_2)\sin\theta \qquad (4)$$

where $\sum F_x$ may take on positive or negative values depending on the relative magnitudes of F_2 and F_6.

Equation (3) yields directly an equation relating the deflection angle, θ_1, to the momenta of the jets. Although the quantities J_1 and J_2 are unknown, they may be determined from experimental data, for example Figure 8. It turns out that both of these quantities vary with respect to their individual inputs J_p and J_c by a constant value. For the case of zero setback, $J_1 \simeq J_p$ and $J_2 = J_c/1.62$. Hence, Equation (3) becomes, including the origin correction indicated in Figure 8,

$$\frac{J_c}{J_p + 200} = 1.62 \left[\frac{1}{\cos\theta} - 1 \right] \qquad (5)$$

For comparison, Equation (5) is represented by the broken lines in Figure 8. Reasonably good agreement is noted. For the most part the differences are well within 5% of the experimentally determined values. Similar results, only the constants differing, were obtained for the other single jet geometries.

To complete the analysis we may now determine the magnitude of the net force from Equation (4). The results are plotted in Figure 16 for three geometries. These results indicate that the net effect of pressure may be a very predominant factor in jet deflection, F_x ranging from about 5 J_c to $-0.5\ J_c$ in the present experiments. When $F_x = 0$ one might say that control is purely by momentum. Negative values of F_x/J_c indicate that F_2 is greater than F_6, a condition that would be expected for large deflection angles.

Because of the questionable validity of the corresponding assumptions in the case of two control jets, no analysis of this case is prescribed, i.e, Equations (1) and (2) hold.

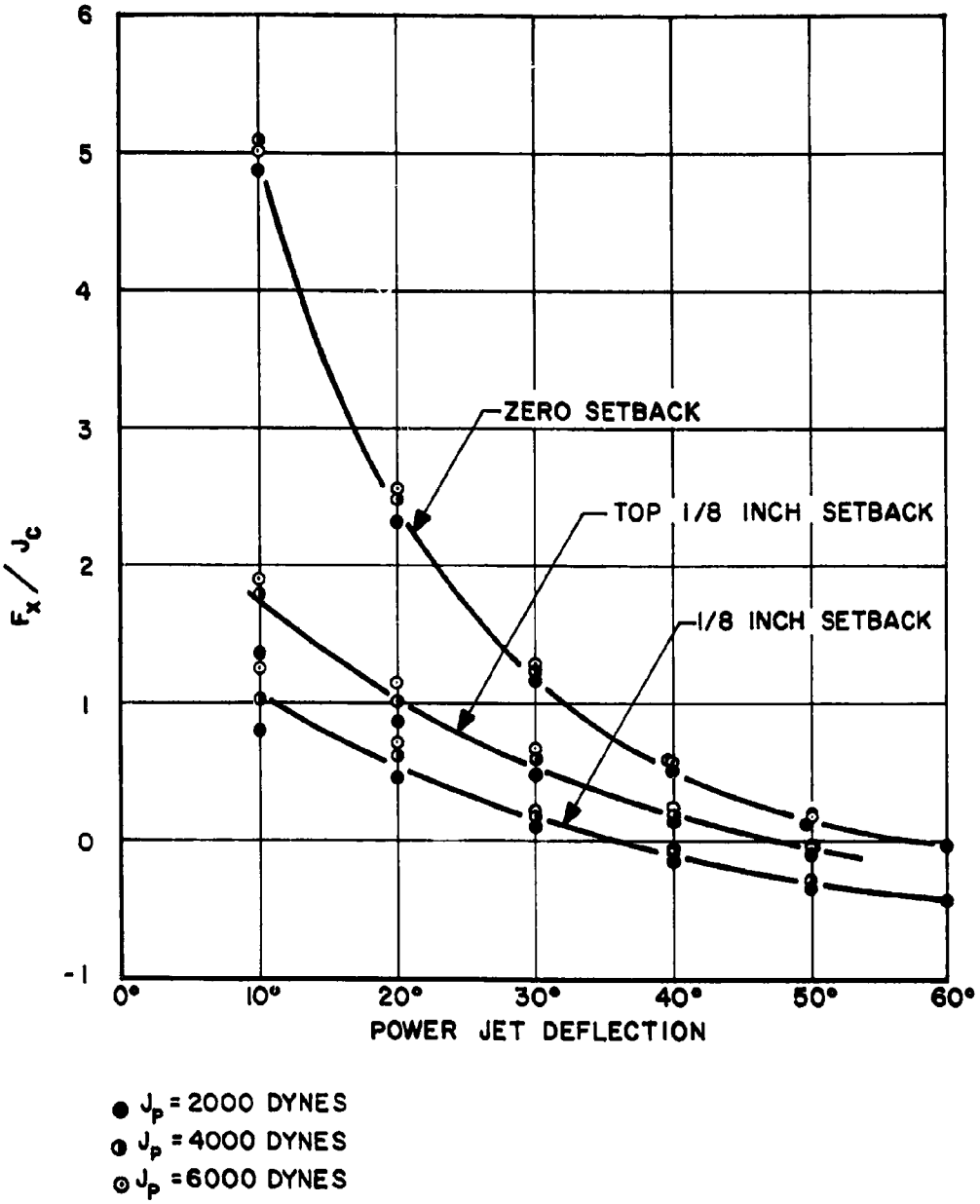

RATIO OF NET PRESSURE FORCE/CONTROL JET MOMENTUM FOR VARIOUS SETBACKS - DEFLECTION BY A SINGLE CONTROL JET

FIGURE 16

V. CERTAIN DYNAMIC ASPECTS

Certain types of fluid jet control devices require that the power jet be rapidly switched between receiver ports to perform a specific function. To gain some insight to the switching response of a fluid jet, a series of experiments were conducted subjecting the power jet to periodic control flows. Both single and opposed control jet configurations were used with disturbance frequencies ranging from zero to about 300 cycles per minute.

Resultant flows took on, more or less, one of two characteristics depending primarily upon the disturbance frequency. These characteristics were as follows, (a) at very low frequencies: the resultant flow in the vicinity of interaction was deflected virtually the same as if the control jet was steady at that instantaneous flow rate (Quasi-Steady Response), (b) at higher frequencies: the combined jet takes on a wavy form, the stability of this form being greatly dependent upon frequency (Dynamic Response).

A. Quasi-Steady Response

If the control jet flow rate is cycled very slowly the resultant jet is almost straight for several power jet slitwidths. As an example, two phases of a particular cycle ($R_p = 258$, $R_{c(max)} = 42$, $f = 3.3$ cycles/min) for defiection by a single jet are shown in Figures 17 and 18. In Figure 17 the control jet has just increased to its maximum moving the jet from the vertical to a deflected position; the movement is from right to left. As the switching action commences a small disturbance to the power jet is created at the point of initial impingement by the control jet. This disturbance then grows and forms a vortex such as shown in Figure 17. The jet remains quite straight upstream of the downstream traveling vortex. As the control jet flow starts to decrease a vortex of opposite rotation forms on the other side of the jet as it commences, to resume its normal position, Figure 18; the movement is from left to right. At the end of the cycle the jet was almost vertical near the orifice; however, the downstream portion did not assume a completely vertical position before thc start of the next cycle.

SINGLE CONTROL JET
PERIODIC FLOW
MOVEMENT RIGHT TO LEFT

$R_p = 258,\ R_{c(max)} = 42$

S = 0.0047

FIGURE 17

SINGLE CONTROL JET
PERIODIC FLOW
MOVEMENT LEFT TO RIGHT

$R_p = 258,\ R_{c(max)} = 42$

S = 0.0047

FIGURE 18

Response to out-of-phase opposed periodic control flows in the quasi-steady regime was quite similar to that for the single jet. Opposed out-of-phase vortex motions resulting from control jet impingement were noted.

It is difficult to assign an upper frequency limit to the region of quasi-steady response since several factors seem significant, among them being R_p, $R_{c(max)}$, the disturbance shape, and the means of application of the disturbance. As a rough estimate, the upper limit appeared to be at about a Strouhal number of 0.08. The significance of the Strouhal number, the non-dimensional wave length of the disturbances, is discussed in the following section.

B. Dynamic Response

Before discussing the results of the present experiments, it would be well to review certain already investigated points concerning the inseparable subject of jet stability. Also of importance is the aspect of dynamic similarity for periodically disturbed jet flows.

It has been noted, for the sensitive jet,* that dynamic similarity of disturbance characteristics does exist, provided that the comparison is made on the basis of both Strouhal number and Reynolds number.[16] The Strouhal number is defined as the product of the disturbance frequency and jet width divided by the mean jet velocity.

$$S = \frac{fW}{U} \tag{7}$$

Physically, we may interpret these two non-dimensional parameters as follows. Reynolds number is important with respect to jet spreading and viscous effects on the disturbance growth while the Strouhal number is proportional to the wave length of the disturbances.

Pertinent results concerning the subject of jet stability may be summarized as follows:[17,18,19]

(1) The degree of instability varies greatly along the length of the jet, the jet being most unstable at the root.

*A jet flow which is very susceptible to impressed disturbances shall be referred to as a sensitive jet.

(2) For small values of S the motion is unstable. As S increases there is a definite boundary defining the upper region of instability.

(3) Instability of the jet increases as the disturbance amplitude increases.

(4) For a given displacement amplitude there is a critical R_p below which the jet is stable at all wave lengths.

(5) As R_p increases the upper boundary of the unstable region is almost at constant S.

Although there are several other details concerning jet stability, the foregoing points should be adequate to allow a more meaningful interpretation of the present experiments. For additional information regarding further analytical and experimental aspects of the subject, the reader is referred to a paper by Chanaud and Powell.[19]

When the flow of the control jet or jets is cycled relatively rapid, two new effects appear. First, because the power jet does not respond instantaneously, some local time averaging effect on deflection must be expected. Second, the resultant jet takes on a wavy form. For a given R_p the stability of this wavy motion is greatly dependent upon the cycling frequency of the disturbance.

As the cycling speed for the single control jet system shown in Figures 17 and 18 was increased, flows such as shown in Figures 19 and 20 resulted. Figure 19 shows the condition of the disturbed jet at $R_p = 258$ and $S = 0.10$ ($f = 73.5$ cycles/min.) Here, the reaction time is still slow enough to deflect the entire jet as can be seen by the step-like discontinuities representing each cycle. The vortex formation is analogous to the quasi-steady case. The rapid growth of the disturbances indicates a marked instability. As the cycling speed is again significantly increased the motion shown in Figure 20 ensues, where $R_p = 258$ and $S = 0.48$ ($f = 340$ cycles/min). In this case the reaction time was so short that the entire jet was not deflected proportionally to the instantaneous control flow rate. Instead, an average deflection resulted and

SINGLE CONTROL JET
PERIODIC FLOW

$R_p = 258$, $R_{c(max)} = 42$

$S = 0.10$

FIGURE 19

SINGLE CONTROL JET
PERIODIC FLOW

$R_p = 258$, $R_{c(max)} = 42$

$S = 0.48$

FIGURE 20

the disturbances to the jet took the form of vortices curling up only on the side of impingement. The condition shown is nearly stable.

For two applied disturbances, i.e., two opposed control jets pulsating out of phase, the dynamic response of the power jet is shown in Figures 21 and 22. As the frequency was increased from the quasi-steady regime, the jet became very unstable. Figure 21 shows this condition for S =0.27. Here, the growth of the disturbance is quite noticeable and the wave peaks due to the applied disturbance break into discrete vortices arranged in an alternate manner. As S is increased still more, a point is reached where the jet finally becomes stable. This condition is shown in Figure 22 for S = 0.71.

A particular point of interest is to define the border between the region of stability and instability (i.e., the neutral stability contour), since this limit occurs in a quite realizable range of frequencies. For the present experiments, neutral stability was defined as the condition of unchanging amplitude of the disturbances lying between 4 and 10 slitwidths from the orifice. The growth of the disturbances must not be confused with the spreading of the jet itself, as may be seen in Figure 22. The disturbed jet displayed what might be called centers of rotation. For experimental neutral stability, between 4 and 10 slitwidths, this rotation was barely noticeable and tended to decay further downstream. For unstable motion the rotation tended to increase with downstream distance.

Contours of neutral stability for three fixed control jet amplitudes are shown in Figure 23. The response of the power jet to the quite different in magnitude disturbances varied considerably. For the smallest disturbance $R_{c(max)} = 19$, the contour of neutral stability was defined by a region of almost constant S except in the lower range of R_p where S tended to gradually increase. For the largest disturbance, $R_{c(max)} = 53$, the contour of neutral stability was defined approximately by a line of constant frequency, i.e., S was nearly linearly dependent on R_p. The frequencies for the points plotted varied less than 8%. The response of the jet to the intermediate disturbance,

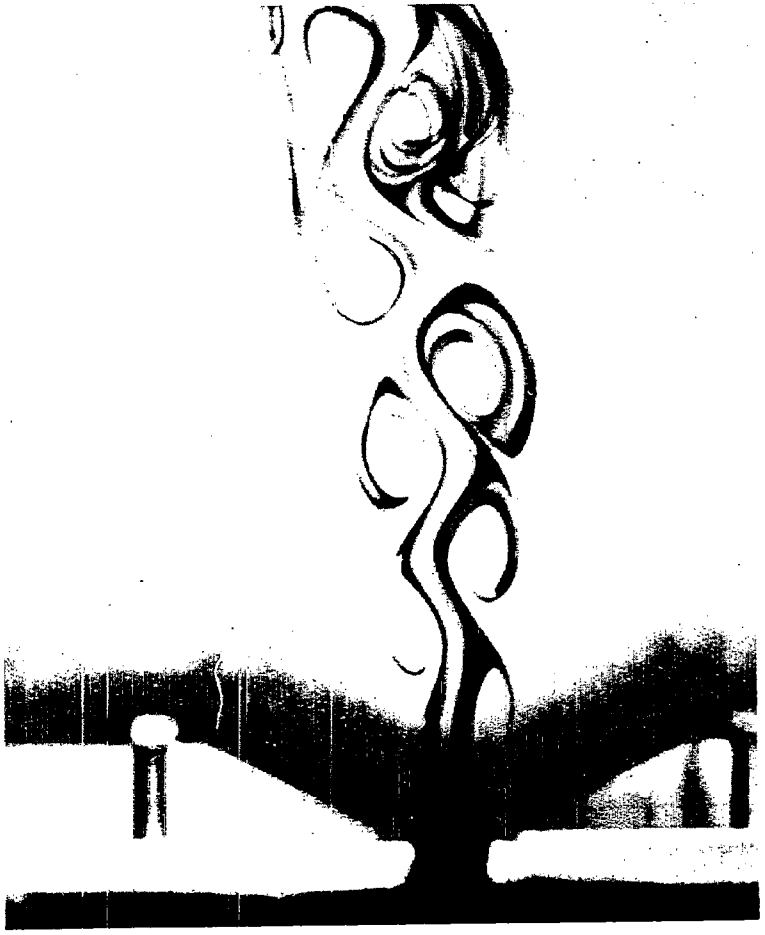

TWO CONTROL JETS
PERIODIC FLOW

$R_p = 80,\ R_{c(max)} = 19$

S = 0.27

FIGURE 21

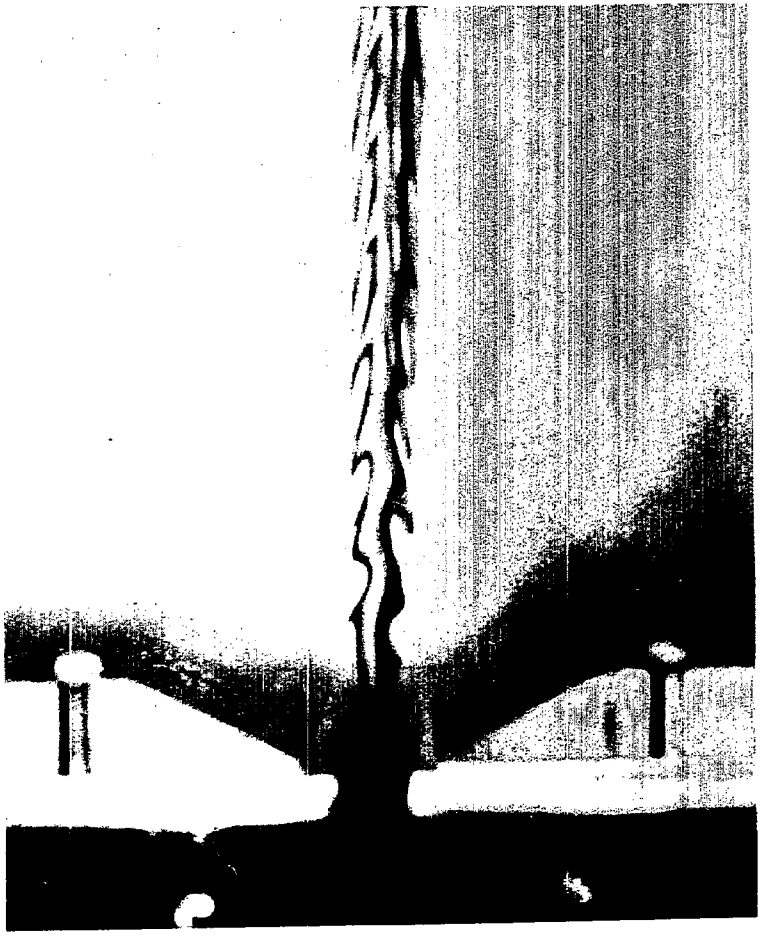

TWO CONTROL JETS
PERIODIC FLOW

$R_p = 80,\ R_{c(max)} = 19$

S = 0.71

FIGURE 22

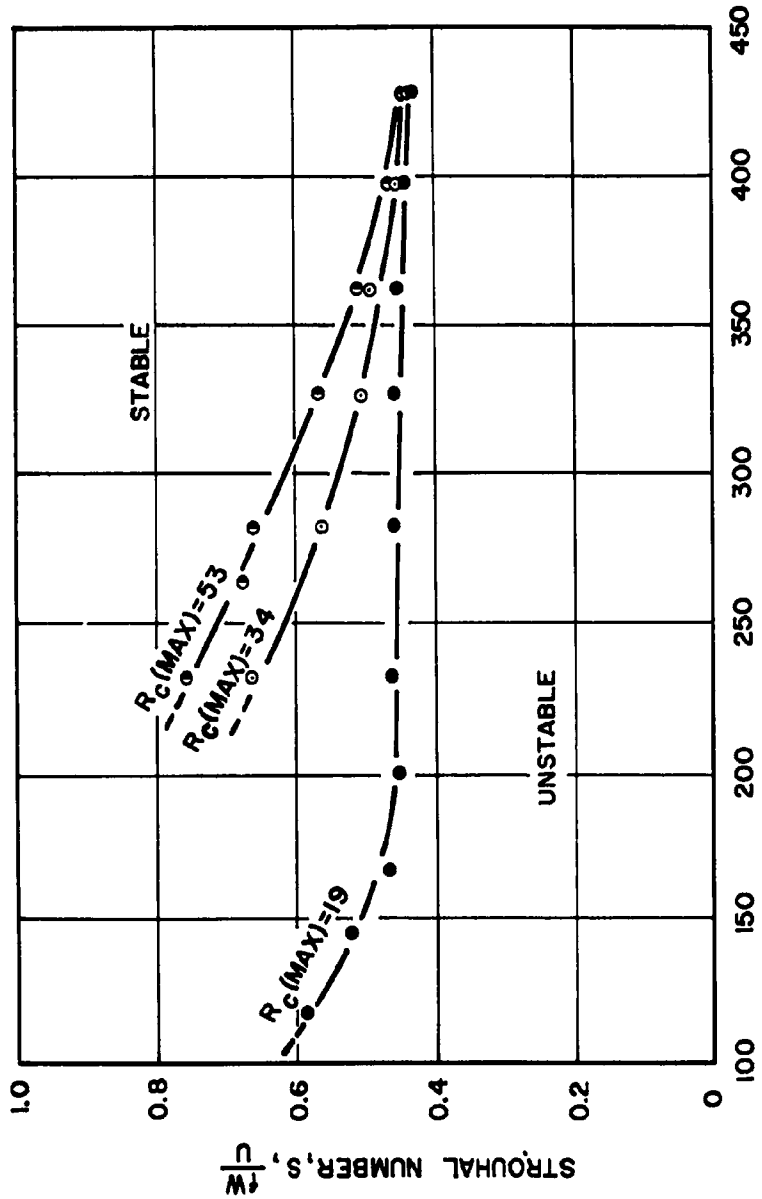

NEUTRAL STABILITY CONTOURS

FIGURE 23

$R_{c(max)}$ = 34, was in between the two boundary cases, both S and frequency varied considerably with R_p.

At low R_p the amplitude of the resultant jet disturbances became so great that the meaning of any observed results was quite questionable. For this reason, experimental measurements for each contour were terminated at the lower limits of R_p indicated in Figure 23.

In the upper range of R_p the neutral stability limit for a relatively wide range of resultant disturbances was bracketed between $0.4 < S < 0.6$. At R_p = 400, the jet appeared rather insensitive to the amplitude of the applied disturbance. Here, the neutral stability limit occurred at about S = 0.45. The general trend was for the stability of the jet to decrease as the amplitude of the applied disturbances increased.

It should be realized that the curves in Figure 23 represent the effect of constant amplitude applied disturbances and not constant resultant displacement of the jet. The displacement, as previously discussed, is some function of the momentum ratio of the jets and reaction time. For constant amplitude displacement of the jet it has been found that neutral stability contours are more or less $\subset$ shaped.[17]

VI. FLOW WITH A WEDGE OBSTACLE IN THE STREAM

Thus far only those flows have been considered where the combined jet is essentially free. If the resultant jet system is to be used in a device, it is practical to harness the flow so that the output signal can be directed to some specific function. This can be accomplished by adding sidewalls and a flow splitter or splitters to form the required array of outputs.

The effect of sidewalls (Coanda effect) was discussed in Section IV, since related phenomena occur to some extent in the presence of the relatively short walls of the control jet body. Although the influence of long walls may become more predominant, the basic qualitative aspects of the flow are essentially the same. However, the presence of a flow splitter, usually in the form of a wedge, presents additional flow features to be studied, namely, the aspects of steady deflection and the dynamic characteristics of the jet as it

traverses the wedge. An additional complication for the case of a wedge present in the jet stream may arise. Under certain conditions, self-excited oscillations of the power jet result.

To study the characteristics of jet deflection with a wedge divider present, measurements were taken to determine the control flow required to just deflect the observable boundaries of the power jet to one side of the wedge. The opposed control jet arrangement with zero setback was used. The wedge elevation h and power jet flow rate expressible as R_p were the controlled variables. The wedge angle was 30 degrees.

The undisturbed flow (control jets inactive) is shown in Figure 24. The power jet is symmetrically bifurcated. Figure 25 shows the observable boundaries of the power jet just completely deflected to one side of the wedge. This is the condition at which the measurements under present consideration were made.

Depending on the elevation of the wedge, or more appropriately the ratio of the wedge elevation to power channel width, h/W_p, there are two means by which the final deflection of the resultant jet may be achieved. These conditions are schematically shown in Figure 26. The distinction is related directly to the magnitudes of the indicated angles, i.e., θ_d(the deflection angle of the jet between the orifice and the edge) and θ_w (the final deflection angle of the jet and half wedge angle).

For a constant half wedge angle, θ_w, if h/W_p is varied, the possibilities $\theta_w \leq \theta_d$ and $\theta_w > \theta_d$ exist. The condition $\theta_w < \theta_d$ arises when h/W_p is small. Here, for the stream to be deflected completely to one side of the wedge it is necessary first to deflect the jet an angle greater than that of the wedge, Figure 26a. As h/W_p is increased, a point is reached where $\theta_w > \theta_d$, then the jet need be deflected only the lesser angle, θ_d. The remainder of the deflection, $\theta_w - \theta_d$, is caused by the wedge. In all cases observed, the resultant flow followed the contour of the wedge.

Experimentally determined control flow requirements to deflect the observable boundaries of the power jet completely to one side of the wedge are

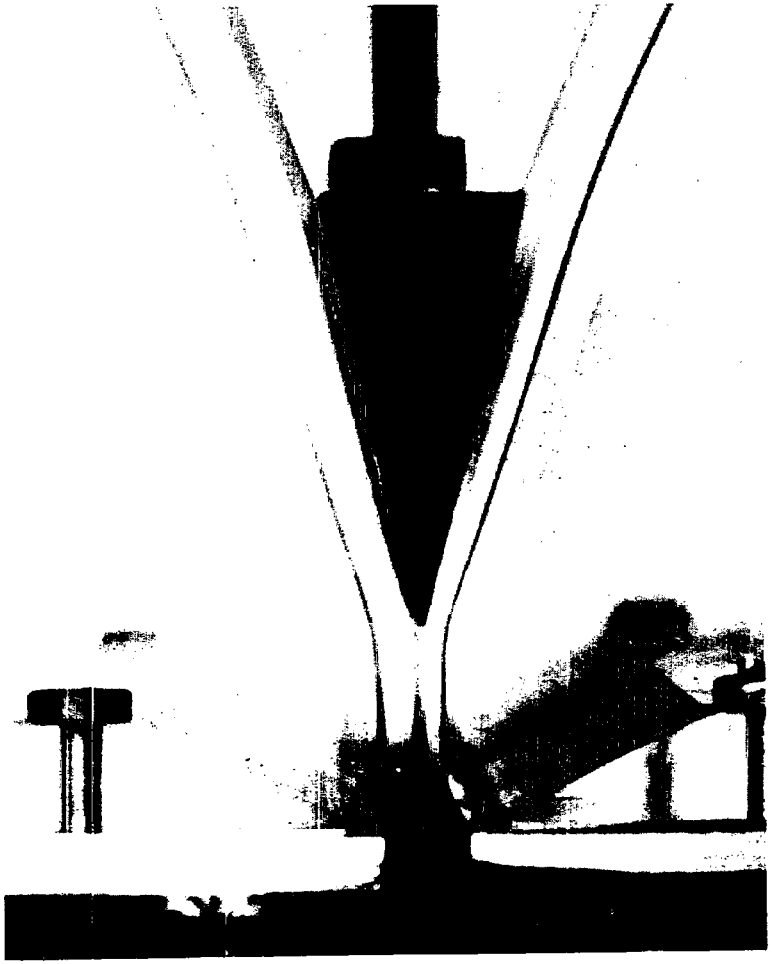

BIFURCATED FLOW
TWO CONTROL JETS

30^{o} Wedge, h = 1.5 cm

$R_p = 200$, $R_c = 0$

FIGURE 24

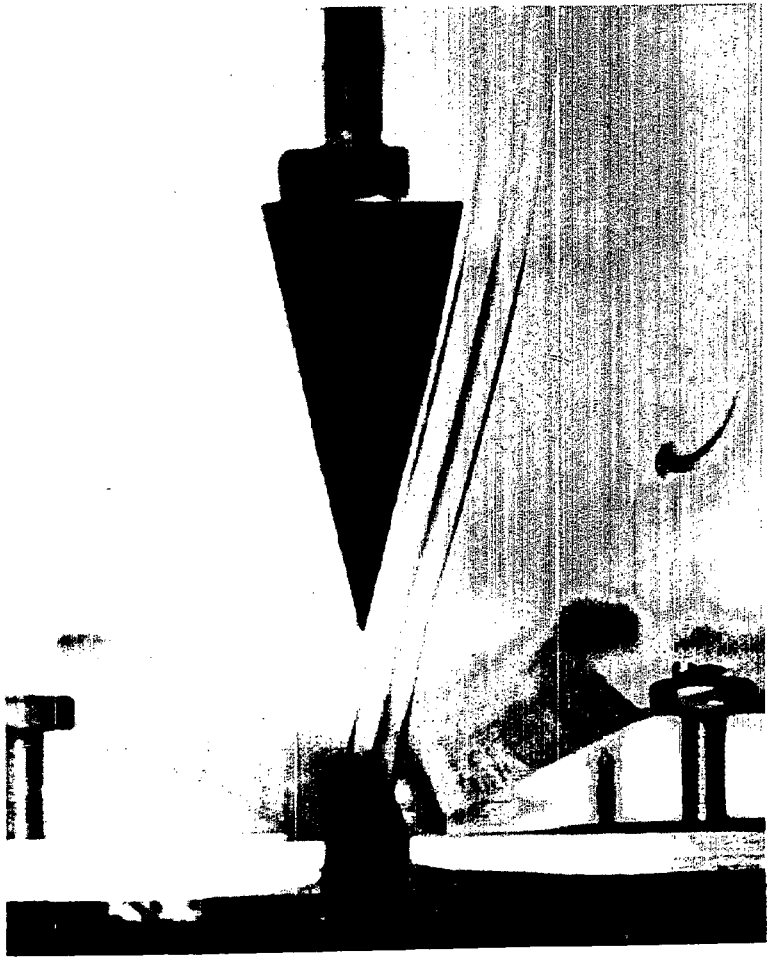

FLOW COMPLETELY DEFLECTED
TWO CONTROL JETS

30^{o} Wedge, h = 1.5 cm

$R_p = 200$, $R_c = 24$

FIGURE 25

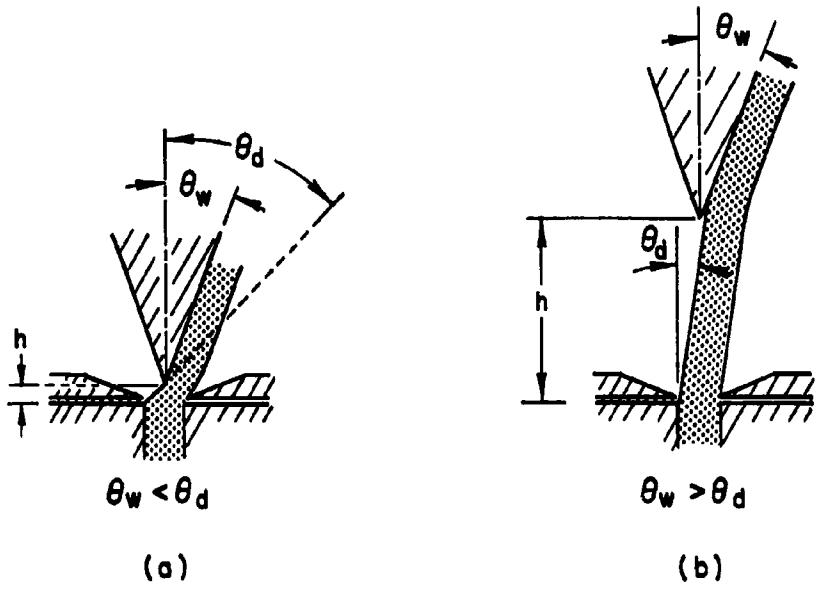

DEFLECTION OF FLOW PAST A WEDGE, DEPENDENCY ON WEDGE HEIGHT ILLUSTRATED

FIGURE 26

shown in Figure 27. Here, the elevation of the wedge was varied for three different power jet flow rates. As would be expected from looking at Figure 26, the control flow requirements increased as h decreased. For a reference, the control flow required to maintain a deflection angle equal to θ_w(30 degrees) with no wedge present is indicated by the dashed line.

A comparison of flow requirements for several points of the jet's traverse showed no noticeable hysteresis tendencies. For example, once the flow was deflected completely to one side of the wedge, a small decrease in control flow would result in essentially immediate response to cause the flow to become split.

When the power jet was dynamically switched with a wedge in the stream, the resultant flow pattern was quite different to that with no wedge present. This difference was primarily due to the fact that additional disturbances result as the jet reacts with the wedge.

Figure 28 shows the flow for dynamic traverse at S = 0.051 (f = 10 cycles/min.), R_p = 140, and $R_{c(max)}$ = 30. This was essentially the quasi-steady regime. Vortices were cast off in alternate sets of four, a set which can be seen to the left of the wedge. The downstream (upper) pair of opposed vortices occurred when the jet switched from left to right past the edge. The upstream (lower) pair also having opposed rotation resulted from the impulse of the control jet.

As the cycling frequency was increased the flow picture became much more complicated. The point was soon reached where the jet displayed considerable curvature between the root and the edge and later where more than one disturbance was present upstream of the edge. This regime was not further investigated as it was outside the scope of the present study.

If the spacing between the orifice and the object in the stream exceeds a certain critical distance, rather violent self-excited oscillations of the power jet result, as may be seen in Figure 29 where the control jets have been removed. This phenomenon is known as the edgetone. The name originates from the sound generation resulting from the fluctuating force of an air jet on a wedge, when the above indicated unstable flow exists.

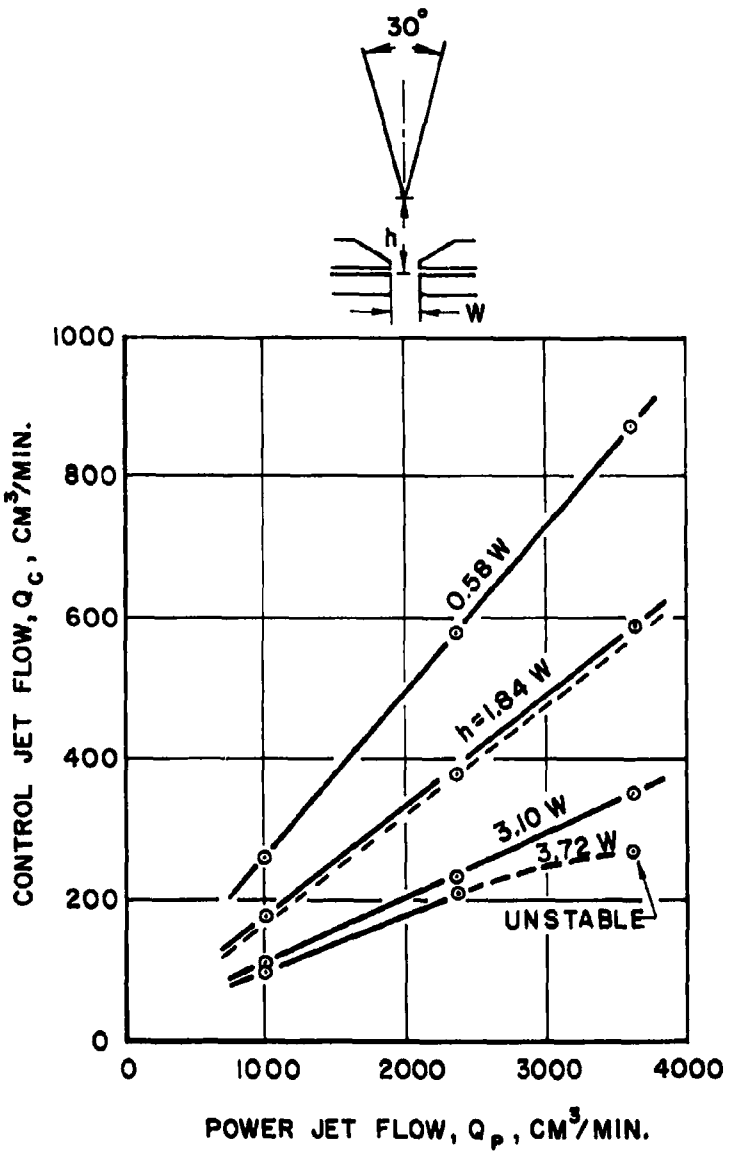

STEADY DEFLECTION PAST A
30 DEGREE WEDGE

FIGURE 27

FORCED OSCILLATIONS

30^{o} Wedge h = 1.5 cm

$R_p = 140$, $R_{c(max)} = 30$

S = 0.051

FIGURE 28

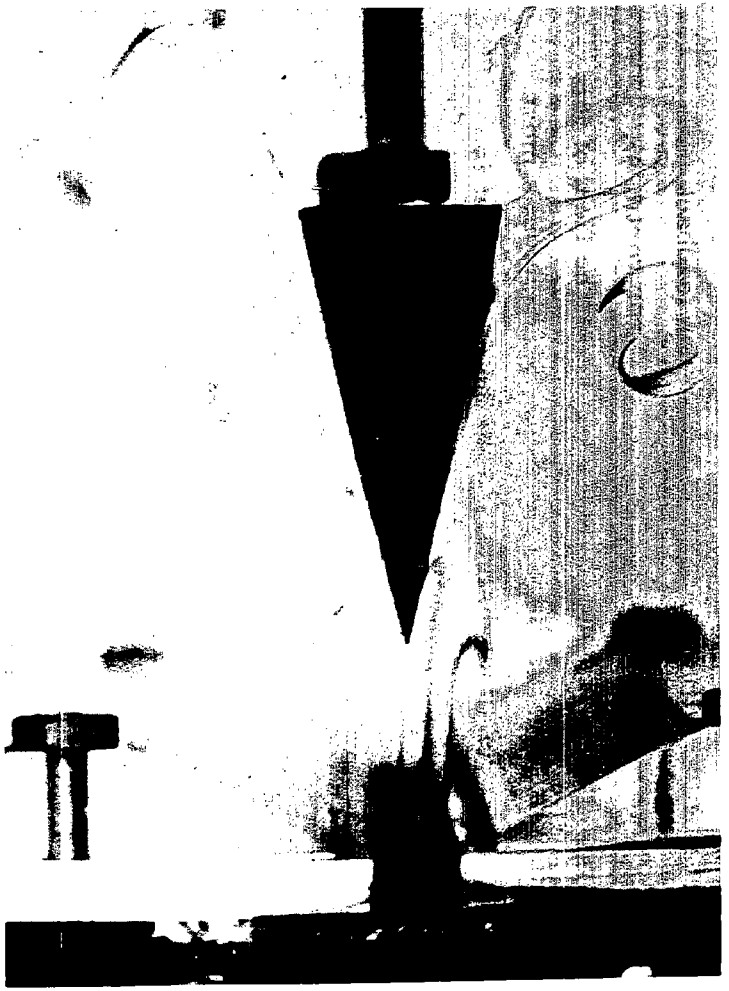

SELF EXCITED OSCILLATIONS

30^{o} Wedge, h = 2.5 cm

$R_p = 240$, S = 0.10

FIGURE 29

The edgetone is the result of a direct feedback of the forces resulting from the fluid interacting with the fixed obstacle.[20,21] The feedback path may be described as follows. Jet disturbances (sinuosities or vortices), interact with the edge resulting in a generated disturbance. The field of this disturbance then results in a traverse disturbance to the jet, which is most sensitive at the orifice. The resultant disturbance to the unstable jet is then amplified, possibly several thousand times, before impingement with the wedge where new disturbances in turn are created. Thus, the feedback loop is established and the motion persists as a constant amplitude periodic process. A more detailed description of the flow field associated with the edgetone phenomenon may be found in the paper by Powell.[22]

In the design of a device, self-excited oscillations may or may not be a desirable feature. In either case, it is important to know the critical orifice-edge distance h_c. For the present experiments this was defined as that distance below which no self-excited oscillations could persist. To ensure that the system was not in a state of pseudo-stability, disturbances were temporarily impressed on the stream. If after the impressed disturbances ceased, the motion died out, the condition of stability was assumed satisfied. Results of experiments for a 30 degree wedge are shown in Figure 30. Some difference in h_c was noted between the two orifice geometries studied. Possibly, the tapered orifice geometry shielded the root of the jet, to some degree, from the disturbance. This would account for the greater stability displayed by this configuration.

Conditions for self-excited oscillations would be expected to be quite altered if the orifice-edge system were placed in a closed device. However, the case for the free jet does give considerable fundamental insight to the general nature of the problem. The designer must be cognizant of the possible outcomes of various wedge positions.

VII CONCLUSIONS

The deflection of a two-dimensional fluid jet by a laterally impinging jet or jets is not only determined by the momenta of the interacting jet system but

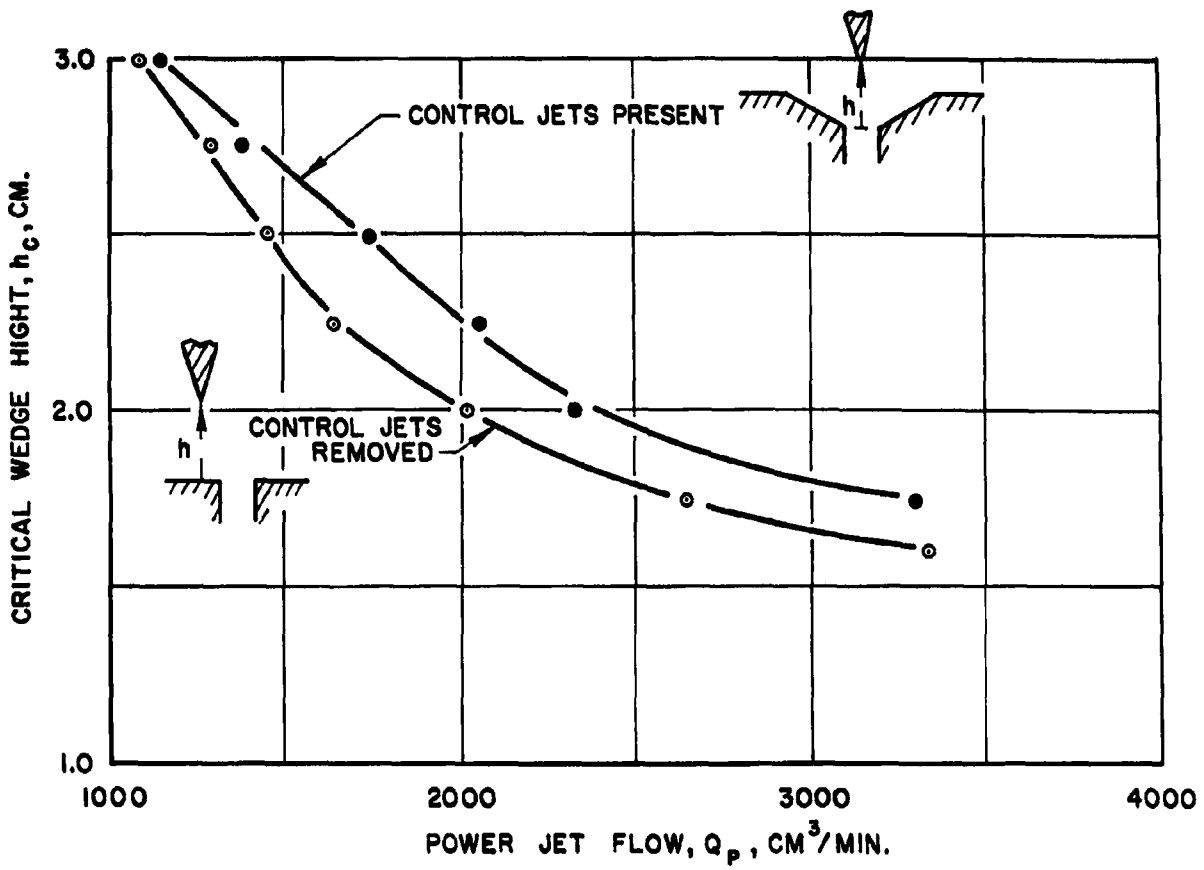

CRITICAL HEIGHT FOR SELF-EXCITED OSCILLATIONS
30 DEGREE WEDGE

FIGURE 30

also the pressure forces resulting from the fluid reacting with nearby solid boundaries. In the case of deflection with only a single control jet present, the geometry shown in Figure 5, experimental results show that the relationship between the momenta of the two input jets is linear for constant angles of deflection. An analysis, centered around a force balance on the system, gives an expression which describes the experimental results with reasonable accuracy. An extension of the analysis indicates that the net pressure forces acting on the jet system may be of significant order of magnitude compared to the momentum forces. For the single control jet geometry, at smaller deflection angles, these pressure forces act in such a direction as to assist in the deflection of the power jet. As the deflection angle is increased, a point is reached where the net pressure force resists deflection.

For a symmetrical geometry, i.e., two oppositely placed control jets, additional pressure forces are introduced. First, the opposing control jet assembly offers greater resistance to deflection. However, if the control jets are set back, a force results which assists deflection. This force is due to the increased velocity of the fluid entrained by the jet in the relatively long and narrow setback cavity, i.e., the Coanda Effect. Results show that there is a particular setback distance at which control flow requirements are a minimum. For the geometry shown in Figure 4, this distance is about 1/2 the power jet width. At this setback distance, control flow requirements to achieve a particular deflection compare favorably to the case for deflection by a single control jet, the most efficient configuration. A comparison for 20 degrees deflection of the power jet for six particular geometries studied is shown in Figure 11.

When the power jet is subjected to dynamic disturbance, i.e., periodic control flows, the resultant flow may be classified into one of two regimes, namely (a) quasi-steady response, where the resultant flow in the vicinity of interaction is deflected virtually the same as if the control is steady at its instantaneous flow rate, and (b) dynamic response, where the jet takes on a definite wavy form. The upper limit for quasi-steady response is at about a Strouhal number of 0.08. The jet is quite unstable when subjected to periodic control flows of intermediate wave length. For shorter wave lengths

the jet becomes stable, neutral stability occurring at about a Strouhal number of 0.5 for disturbances of moderate amplitude.

The presence of a wedge divider centered in the stream introduces new parameters critical in defining the resultant flow. If the control jets are inactive and the wedge height short, less than about 6 slitwidths in the present experiments for $R_p < 425$, the flow is merely bifurcated. However, as the wedge height is increased, a certain critical distance exists where self-excited oscillations ensue. This critical height decreases as the Reynolds number of the jet increases.

For stable conditions, the ratio of the input momenta required for steady deflection of the power jet just past the wedge is essentially constant. Control flow requirements do, however, increase as wedge height is decreased. For dynamic deflection past a wedge the observed flow appears quite complicated. This is due partly to the waviness of the jet between the orifice and edge and also the resultant vortex formations which result as the jet traverses the wedge.

REFERENCES

1. "News Release" Wednesday, 2nd March 1960. Diamond Ordnance Fuze Laboratories (Reference Public Relations Officer J. Wheeler) Parts a through f.

2. Kompass, E.J., "The State of the Art in Fluid Amplifiers", Control Engineering, 10 (1):88-93, Jan. 1963.

3. Wuerer, J.E., The Control of Jets by Auxiliary Flows, M.S. Thesis, Dept. of Engineering, University of California, Los Angeles, June 1963.

4. Powell, A., "Characteristics and Control of Free Laminar Jets", Proceedings of the Fluid Amplification Symposium, Diamond Ordnance Fuze Laboratories, Washington, D.C., 1962, 1:289-299.

5. Indrikis, J., and Powell, A., unpublished work.

6. Bickley, W.G., "The Plane Jet", Phil. Mag., Ser. 7, 23:727-731, April 1937.

7. Gortler, H., "Berechnung von Aufgaben der Freien Turbulence auf Grund eines neuen Näherungsansatzes", ZAMM, 22:244-254, 1942.

8. Chanaud, R.C., and Powell, Alan, "Experiments Concerning the Sound-Sensitive Jet", J. Acoust. Soc. Am., 34:907-915, July 1962.

9. Foerthmann, E., "Über turbulente Strahlausbreitung", Ing.-Arch., 5: p. 42, 1934; also NACA TM-789, 1936.

10. Coanda, H., Patent No. 788, 140 (France) 217, 1934, "Precede et dispositif pour faire devier, une veine fluide penetrant autre fluids."

11. Sawyer, R.A., "The Flow due to a Two-Dimensional Jet Issuing Parallel to a Flat Plate", J. Fluid Mech., 9:543-560, Dec. 1960.

12. Borque, C., and Newman, B.G., "Reattachment of a Two-Dimensional Jet to an Adjacent Flat Plate", Aero. Quat. 11:201-232, Aug. 1960.

13. Crossley, R.W., "Basic Research and Development in Fluid Power Control for U.S.A.F. for the Period 1 February 1961 to 31 May 1961", Dynamic Analysis and Control Laboratory, Massachusetts Institute of Technology, ASD-TR 61-349.

14. Brown, F.T., Pneumatic Pulse Transmission with Bi-stable Jet-Relay Reception and Amplification, Sc. D. Thesis, Dept. of Mech. Engr., Massachusetts Institute of Technology, May 1962, Chapter 8.

15. Milne-Thomson, L.M., Theoretical Hydrodynamics, 4th Ed., Macmillan Company, New York, 1960, p. 290.

16. Powell, A., Noise of Jets, Ph.D. Thesis, University of Southhampton, England, 1953.

17. Rayleigh, 3rd Baron (John William Strutt), Theory of Sound, Dover New York, 1945, Vol. 2, Chapter 21.

18. Brown, G.B., "On Vortex Motion in Gaseous Jets and the Origin of Their Sensitivity to Sound", Proc. Phys. Soc. London, 47:703-732, July 1935.

19. Chanaud, R.C., and Powell, Alan, "Experiments Concerning the Sound-Sensitive Jet", J. Acoust. Soc. Am., 34:907-915, July 1962.

20. Powell, A., "On Edge Tones and Associated Phenomena", Acustica, 3:233-243, 1953.

21. Powell, A., "On the Edgetone", J. Acoust. Soc. Am., 33 (4):395-409, April 1961.

22. Powell, A., "Nature of the Feedback Mechanism in Some Fluid Flows Producing Sound", Proceedings of the Fourth International Congress on Acoustics, Copenhagen, 1962.

DISTRIBUTION LIST

Agency	Copies
Chief of Naval Research Department of the Navy Washington 25, D. C.	
Attn: Codes 438	3
461	1
463	1
466	1
468	1
Commanding Officer Office of Naval Research Branch Office 495 Summer Street Boston 10, Massachusetts	1
Commanding Officer Office of Naval Research Branch Office 86 East Randolph Street Chicago 1, Illinois	1
Commanding Officer Office of Naval Research Branch Office 207 West 24th Street New York 11, New York	1
Commanding Officer Office of Naval Research Branch Office Navy #100, Box 39 Fleet Post Office New York, New York	25
Commanding Officer Office of Naval Research Branch Office 1030 East Green Street Pasadena 1, California	1
Commanding Officer Office of Naval Research Branch Office 1000 Geary Street San Francisco 9, California	1
Director Naval Research Laboratory Washington 25, D.C.	
Attn: Codes 2000	1
2020	1
2027	6
Chief, Bureau of Ships Department of the Navy Washington 25, D.C.	
Attn: Codes 305	1
335	1
341	1
345	1
421	1
Chief, Bureau of Naval Weapons Department of the Navy Washington 25, D.C.	
Attn: Codes R-12	1
RR	1
RU	1
Commanding Officer and Director David Taylor Model Basin Washington 7, D.C.	
Attn: Codes 142	1
513	1
550	1
Fluid Motion & Sound (1) 6/25/63	

Agency	Copies
Commander Naval Ordnance Laboratory Silver Spring, Maryland	
Attn: Desk HL	1
Commander U.S. Naval Ordnance Test Station Pasadena Annex 3202 E. Foothill Boulevard Pasadena 8, California	
Attn: Research Division	1
P508	1
Mr. J. W. Hoyt	
Commander Naval Ordnance Test Station China Lake, California	
Attn: Mr. J. W. Hicks	1
Superintendent U.S. Naval Academy Annapolis, Maryland	
Attn: Library	1
Commanding Officer and Director U. S. Naval Engineering Experiment Station Annapolis, Maryland	
Attn: Code 750	1
Commanding Officer NROTC and Naval Administrative Unit Massachusetts Institute of Technology	
Cambridge 39, Massachusetts	1
Commanding Officer and Director Underwater Sound Laboratory Fort Trumbull New London, Connecticut	
Attn: Technical Library	1
Commanding Officer and Director U. S. Navy Mine Defense Laboratory	
Panama City, Florida	1
Superintendent U.S. Naval Postgraduate School Monterrey, California	
Attn: Library	1
Commanding Officer and Director Naval Electronic Laboratory San Diego 52, California	
Attn: Code 4223	1
Commander Norfolk Naval Shipyard	
Portsmouth, Virginia	1
Commander New York Naval Shipyard Naval Base	
Brooklyn, New York	1
Commander Boston Naval Shipyard	
Boston 29, Massachusetts	1
Commander Philadelphia Naval Shipyard Naval Base	
Philadelphia 12, Pennsylvania	1
Commander Portsmouth Naval Shipyard Portsmouth, New Hampshire	
Attn: Design Division	1

Agency	Copies
Commander Charleston Naval Shipyard U.S. Naval Base Charleston, South Carolina	1
Commanding Officer Long Beach Naval Shipyard Long Beach 2, California	1
Commanding Officer U.S. Naval Underwater Ordnance Station Newport, Rhode Island Attn: Research Division	1
Commander Pearl Harbor Naval Shipyard Navy #128, Fleet Post Office San Francisco, California	1
Commander San Francisco Naval Shipyard San Francisco 24, California	1
Commander Mare Island Naval Shipyard Vallejo, California	1
Commanding Officer U.S. Army Research Office Box CM, Duke Station Durham, North Carolina	1
Commander Hdqs. U.S. Army Transportation Research & Development Command Transportation Corps Fort Eustis, Virginia	1
Office of Technical Services Department of Commerce Washington 25, D.C.	1
Defense Documentation Center Arlington Hall Station Arlington 12, Virginia	10
Fluid Mechanics Section National Bureau of Standards Washington 25, D.C. Attn: Dr. G. B. Schubauer	1
Director Langley Research Center National Aeronautics and Space Administration Langley Field, Virginia	1
Director Ames Research Laboratory National Aeronautics and Space Administration Moffett Field, California	1
Director Lewis Research Center National Aeronautics and Space Administration Cleveland, Ohio	1
Director Engineering Science Division National Science Foundation Washington, D.C.	1
Air Force Office of Scientific Research Mechanics Division Washington 25, D.C.	
National Academy of Sciences National Research Council 2101 Constitution Avenue, NW Washington 25, D.C.	1
Engineering Societies Library 29 West 39th Street New York 18, New York	1

Agency	Copies
Society of Naval Architects and Marine Engineers 74 Trinity Place New York 6, New York	1
Webb Institute of Naval Architecture Glen Cove, Long Island, New York Attn: Technical Library Professor E. V. Lewis	1 1
Institute of Mathematical Sciences New York University 25 Waverly Place New York 3, New York Attn: Professor J. J. Stoker	1
The Johns Hopkins University Baltimore 18, Maryland Attn: Professor O. M. Phillips Professor S. Corrsin	1 1
Director Applied Physics Laboratory The Johns Hopkins University 8621 Georgia Avenue Silver Spring, Maryland	1
California Institute of Technology Pasadena 4, California Attn: Hydrodynamics Laboratory Professor T. Y. Wu Professor A. Ellis	1 1 1
University of California Berkeley 4, California Attn: Department of Engineering Professor J. V. Wehausen Professor H. A. Schade Professor E. V. Laitone	1 1 1 1
Iowa Institute of Hydraulic Research State University of Iowa Iowa City, Iowa Attn: Professor H. Rouse Professor L. Landweber	1 1
Harvard University Cambridge 38, Massachusetts Attn: Professor G. Birkhoff Professor G. F. Carrier Professor S. Goldstein	1 1 1
University of Michigan Ann Arbor, Michigan Attn: Engineering Research Institute Professor W. W. Willmarth	1 1
Director Ordnance Research Laboratory Pennsylvania State University University Park, Pennsylvania Attn: Dr. E. J. Skudrzyk Dr. G. F. Wislicenus Dr. M. Sevik	1 1 1
Director St. Anthony Falls Hydraulic Laboratory University of Minnesota Minneapolis 14, Minnesota Attn: Professor B. Silberman Professor L. G. Straub	1 1
Massachusetts Institute of Technology Cambridge 39, Massachusetts Attn: Professor P. Mandel Professor C. C. Lin Professor M. A. Abkowitz Professor Mollo-Christensen Professor M. Landahl	1 1 1 1 1
Institute for Fluid Mechanics and Applied Mathematics University of Maryland College Park, Maryland Attn: Professor J. M. Burgers	1

Agency	Copies
Graduate School of Aeronautical Engineering Cornell University Ithaca, New York Attn: Professor W. R. Sears	1
Brown University Providence 12, Rhode Island Attn: Dr. R. E. Meyer	1
Stevens Institute of Technology Davidson Laboratory Hoboken, New Jersey Attn: Dr. S. J. Lukasik Mr. D. Savitsky Mr. J. P. Breslin	1 1 1
Department of Mathematics Rensselaer Polytechnic Institute Troy, New York Attn: Professor R. C. DiPrima	1
Southwest Research Institute 8500 Culebra Road San Antonio 6, Texas Attn: Dr. H. N. Abramson	1
Department of Aeronautical Engineering University of Colorado Boulder, Colorado Attn: Professor M. S. Uberoi	1
Dr. R. H. Kraichnan 425 Riverside Drive New York 25, New York	1
Dr. A. Ritter Therm Advanced Research Division Therm, Incorporated Ithaca, New York	1
Dr. Ira Dyer Bolt, Beranek, and Newman, Inc. 50 Moulton Street Cambridge, Massachusetts	1
Hydronautics, Incorporated Pindell School Road Howard County Laurel, Maryland Attn: Mr. P. Eisenberg, President Mr. M. P. Tulin, V. P.	1 1
Dr. J. Kotik Technical Research Group, Inc. 2 Aerial Way Syosset, New York	1
Director Hudson Laboratories Dobbs Ferry, New York	1
Armour Research Foundation Illinois Institute of Technology Chicago 16, Illinois Attn: Library	1
Oceanics, Incorporated Plainview, Long Island, New York Attn: Dr. Paul Kaplan	1
Dr. B. Sternlicht Mechanical Technology Incorporated 968 Albany-Shaker Road Latham, New York	1
University of California Los Angeles, California Attn: Professor A. Powell	1